4-2017

Modeling Gross Primary Production of Midwest Maize and Soybean Croplands with Satellite and Gridded Weather Data

Gunnar Malek-Madani
University of Nebraska - Lincoln, gunnarmm5@gmail.com

MODELING GROSS PRIMARY PRODUCTION OF MIDWEST MAIZE AND SOYBEAN CROPLANDS WITH SATELLITE AND GRIDDED WEATHER DATA

By

Gunnar Malek-Madani

A Thesis

Presented to the Faculty of

The Graduate College at the University of Nebraska

In Partial Fulfillment of Requirements

For the Degree of Master of Arts

Major: Geography

Under the Supervision of Professor Elizabeth Walter-Shea

Lincoln, NE

April, 2017

Modeling Gross Primary Production of Midwest Maize and Soybean Croplands with Satellite and Gridded Weather Data

Gunnar Malek-Madani, M.A.

University of Nebraska, 2017

Advisor: Elizabeth A. Walter-Shea

The gross primary production (GPP) metric is useful in determining trends in the terrestrial carbon cycle. Models that determine GPP utilizing the light use efficiency (LUE) approach in conjunction with biophysical parameters that account for local weather conditions and crop specific factors are beneficial in that they combine the accuracy of the biophysical model with the versatility of the LUE model. One such model developed using *in situ* data was adapted to operate with remote sensing derived leaf area index (LAI) data and gridded weather datasets. The model, known as the Light Use Efficiency GPP Model (EGM), uses a four scalar approach to account for biophysical parameters including temperature, water stress, light quality, and phenology. The model was calibrated for four locations (seven fields) in the northern Midwest and was driven using remotely sensed LAI data and gridded weather data for these locations. Results showed reasonable error estimates (RMSE = 3.5 g C m^{-2} d^{-1}). However, poor gridded weather atmospheric pressure and incoming solar radiation inputs, increased climatic variation in the study sites and contributed to higher RMSE that observed when the model was applied exclusively to *in situ data* from the Nebraska sites (2.6 g C m^{-2} d^{-1}). Additionally, the application of LAI algorithms calibrated using solely Nebraska sites to sites in Iowa, Minnesota, and Illinois without verification of their

accuracy potentially lead to increased error. Despite this, the study showed there is good correlation between measured and modeled GPP using this model for the field years under study. As the ultimate objective of research is to develop regional estimates of GPP, the decrease in model accuracy is somewhat offset by the model's ability to function with gridded weather datasets and remotely sensed biophysical data.

Acknowledgments

Above all I would like to acknowledge the incredible amount of support I received from Dr. Elizabeth Walter-Shea, my graduate adviser. Dr. Walter-Shea not only made graduate school a possibility for me by taking me on as a student, she ensured that I was successful by taking the time out of her schedule to meet with me every week, helping me to navigate the often confusing environs of graduate school, and inspiring me with her tenacious dedication to her craft. Over the course of this project she provided invaluable guidance, insight, and knowledge. Simply put, neither this project specifically nor my graduate studies in general would have been successful without her.

I would like to thank my entire committee for their tireless support as well: Dr. Anthony Nguy-Robertson, Dr. Andrew Suyker, and Dr. David Wishart. This project was complex and data intensive and without their knowledge and experience it would never have even gotten off the ground. Much of the groundwork for my thesis was laid by Dr. Nguy-Robertson and Dr. Suyker long before I had a hand in things, and I greatly appreciate their trust in allowing me to take the reins for the latest iteration of the overall project. I would like to thank Dr. Wishart, a brilliant geographer and author, for providing me with a geographic lens through which to focus my studies and writing.

I would also like to thank Dr. Katherine Nashleanas, Dr. Brian Wardlow, and Dr. Rong Yu for trusting me in assisting with their classes during my tenure at UNL. Helping

to teach their classes forced me to better learn my subject of study and I will take the experience gained through teaching with me throughout my career.

I am thankful for the support of the staff at UNL for their endless administrative and technical assistance, my fellow graduate students for showing me the ropes and sharing in this experience with me, and to all of the great professors in SNR, Geography, and Agronomy who taught me so much about the natural world. The community at UNL truly is special.

Lastly, I am incredibly grateful for the support of my wonderful family including my parents, Joe and Terri, my sister Kristen, my beautiful and intelligent wife Carrie, and our daughter Eleanor.

Table of Contents

CHAPTER 1 INTRODUCTION

Gross primary production (GPP) in maize and soybean crops at a landscape level is an important measure for quantifying large scale carbon flux or plant productivity. GPP is defined as the total amount of organic matter produced due to photosynthesis in a defined area over a unit of time (Gitelson et al., 2006). GPP is a useful metric in determining the patterns and dynamics of the terrestrial carbon cycle (Cui et al., 2016), and it is essential in the study of ecosystem respiration and biomass accumulation (Beer et al., 2010). The need to quantify the North American carbon sink necessitates precise carbon dioxide flux measurements (Suyker and Verma, 2012) and while *in situ* data sources are available for this quantification, they represent field level data collection at specific locations. Therefore, GPP determination at the regional scale can help determine large scale patterns and dynamics of the ecological system and help to quantify long term carbon trends. Models have been created in an attempt to derive an accurate estimation of GPP at the landscape level with varying degrees of accuracy (e.g., Matsushita and Tamura., 2002 [20% error]; Heinsch et al., 2003 [18% error]; Heinsch et al., 2006 [20%-30%]; Xiao et al., 2004; Cui et al., 2016 [Root Mean Square Error (RMSE) = 2.97 g C m^{-2} d^{-1}]). These landscape models use respective regional input data to generate estimates of GPP at course temporal scales over a range of managed and unmanaged ecosystems.

In estimating GPP on a regional scale, the use of satellite imagery and modeled weather data is essential as monetary, personnel, time, and equipment constraints

hinder the collection of daily *in situ* data. As a result, there is a push to develop new, and adapt proven, GPP models to function accurately with satellite and modeled weather data as input (Cui et al., 2016), although many of these models also do not estimate GPP at a daily temporal resolution. While the overall accuracy of these adjusted models may currently be lower than those that utilize *in situ* field-level input, due in part to the generalization of model parameters to work on heterogeneous regions, the spatial and temporal restrictions of satellite data, and the accuracy of modeled weather input data, the ability to study large regions may offset the loss of accuracy depending upon the scope and objectives of the research being conducted (Cui et al., 2016; Matsushita and Tamura., 2002). The quality of the remotely sensed and modeled weather inputs in GPP models is directly tied to the accuracy in estimating GPP (Matsushita and Tamura, 2002), therefore it is of equal importance that accurate input data are utilized by the researcher.

In 2015, a light use efficiency model, known as the Light use Efficiency GPP Model (EGM), was introduced by Nguy-Robertson et al. (2015). The model is essentially a hybrid of Monteith's (1972) light use efficiency relationship with elements of eco-physiological models (Reich et al., 1991; Kalfas et al., 2011; Suyker and Verma, 2012; Gilmanov et al., 2013). Nguy-Robertson et al. (2015) used *in situ* data inputs including destructive leaf area and meteorological measurements. This model takes into account the effects that environmental and canopy factors (light quality, water availability, temperature, and phenology) have on photosynthesis in maize and soybean plants. The

EGM uses daily weather inputs and information on photosynthesizing leaf material (green leaf area) to estimate plant photosynthesis under varying environmental conditions. Previously developed GPP models use a maximum (constant) light use efficiency (ε_0) input in modeling GPP which, as environmental conditions change, can be downregulated (e.g. Heinsch et al., 2003; Xiao et al., 2004; Li et al., 2012; Cui et al., 2016). The EGM uses scalars to account for water stress, daily temperature, amount of diffuse light, and phenology, using green leaf area index (gLAI) as a proxy, in such a way that instead of using solely a maximum ε_0 value, ε_0 is used in conjunction with the scalars to produce a more descriptive daily light use efficiency (ε). This variable can increase with increased diffuse lighting conditions and decrease with environmental stress. For example, increases in diffuse lighting will increase light use efficiency while added stressors due to less optimal temperature, water stress, and plant age can decrease light use efficiency. Nguy-Robertson et al. (2015) drove this model using *in situ* mass and energy flux measurements, micrometeorological observations and leaf area measurements specific to each individual study site to determine the scalars which drive the EGM to simulate daily GPP for three research fields in southeastern Nebraska. The model yielded results that were more accurate than achieved with a previous model that incorporated diffuse lighting effects alone on GPP (e.g. Suyker and Verma, 2012). The EGM of Nguy-Robertson et al. (2015) improved the bias error of the Suyker and Verma model (2012) (RMSE of 2.6 g C m^{-2} d^{-1} and a Mean Normalized Bias (MNB) of 1.7% compared to an RMSE of 3.1 g C m^{-2} d^{-1} and an MNB of 12.5%).

As a means toward the goal of daily, regional GPP estimates, the objective of this study is to employ the enhanced four-scalar light use efficiency approach of Nguy-Robertson et al. (2015) to demonstrate its applicability in using input data derived from remotely sensed and gridded weather datasets to estimate daily GPP over the entire growing season in seven northern Midwest agricultural sites located in Mead, Nebraska, Rosemont, Minnesota, Brooksfield, Iowa and Bondville, Illinois. An analysis of the resulting daily GPP estimates was then conducted to determine how well the EGM functioned using the adjusted input data and study sites.

CHAPTER 2 METHODS

Locations and Attributes of Study Sites

Seven Midwestern agricultural sites from the AmeriFlux network were used in this study (Table 1). All sites are characterized by a humid continental climate (Dfa Koeppen climate classification) with hot humid summers and severe cold winters. Three of the sites are located in southeastern Nebraska (US-Ne1, US-Ne2, and US-Ne3), one in Illinois (US-Bo1), two in Iowa (US-Br1 and US-Br3) and one in Minnesota (US-Ro1) (Table 1). The Nebraska sites are located at the University of Nebraska's Agricultural and Development Research Center near Mead, NE. US-Ne1 (41.1650°N, 96.4766°W, 361m), and US-Ne2 (41.1650°N, 96.4700°W, 362m) are irrigated while US-Ne3 (41.1797°N, 96.4396°W, 363 m) is rainfed. The three Nebraska sites are located roughly 40 km northeast of Lincoln. US-Ne1 and US-Ne2 are adjacent to one another while US-Ne3 is located approximately 3 km to the northeast of US-Ne1 and US-Ne2. All three sites have been under no-till management save for an initial disking conducted in 2001. Since 2005 a conservation-plow tillage has been in effect at US-Ne1 (only). US-Ne1 is planted with maize every year with no rotation between crop types. US-Ne2 and US-Ne3 both have a maize-soybean rotation (maize planted on odd numbered years and soybean planted on even numbered years) except in 2010 and 2012 when US-Ne2 was planted with maize. The mean annual temperature at the three sites is approximately 10°C and the mean annual precipitation for the three sites is approximately 790mm.

US-Bo1 (40.0062°N, 88.2904°W, 219m) is located approximately seven miles south of Champaign, Illinois. The site is not irrigated and is under no-till management administered by NOAA. US-Bo1 alternates annually between maize and soybean crops, with maize cultivation on odd years and soybean cultivation on even years. US-Bo1 has a mean annual temperature of 11°C and a mean annual precipitation of 991mm.

The two Iowa Brooksfield sites, US-Br1 (41.9749°N, 93.6906°W, 313m) and US-Br3 (41.9747°N, 93.6935°W, 313m), are located directly adjacent to one another approximately five miles southwest of Ames, Iowa. Neither field is irrigated while they are both under a tillage management system overseen by the USDA. Both fields at the site are under an annual maize-soybean rotation; US-Br1 is cultivated with maize in odd years and soybean in even numbered years, while US-Br3 is cultivated with soybean in odd numbered years and maize on even numbered years. The mean annual temperature at the two fields is approximately 9°C and the mean annual precipitation is approximately 845mm.

The Minnesota Rosemont site, US-Ro1 (44.7143°N, 93.0898°W; 290 m), is located approximately 24 km south of Saint Paul, Minnesota. This field is not irrigated but is under chisel plow tillage management in the fall succeeding maize harvest and in the spring following soybean harvest in the fall. The US-Ro1 is managed jointly by the University of Minnesota and the USDA. Crop type is alternated annually between maize and soybean, with maize being planted on odd numbered years and soybeans being

planted on even numbered years. The mean annual temperature is 6°C and the mean annual precipitation is 879mm.

Table 1: Ameriflux study sites with crop rotations and management status

Location	Site	Lat., Long.	Mgmt.	Maize crop	Soybean crop
Mead, NE	US-Ne1	41.1650°N, 96.4766°W, 361m	Irrigated	2002-2013	--
	US-Ne2	41.1650°N, 96.4700°W, 362m	Irrigated	2003-2013 Odd Years; 2010, 2012	2002-2008 Even years
	US-Ne3	41.1797°N, 96.4396°W, 363 m	Rainfed	2003-2013 Odd Years	2002-2012 Even years
Brooksfield, IA	US-Br1	41.9749°N, 93.6906°W, 313m	Rainfed	2005-2011 Odd Years	2006-2010 Even Years
	US-Br3	41.9747°N, 93.6935°W, 313m	Rainfed	2006-2010 Even Years	2005-2011 Odd years
Bondville, IL	US-Bo1	40.0062°N, 88.2904°W, 219m	Rainfed	2001-2007 Odd Years	2002-2006 Even years
Rosemont, MN	US-Ro1	44.7143°N, 93.0898°W; 290 m	Rainfed	2005-2011 Odd Years	2006-2012 Even years

Input Data

Daymet Data

Weather data were obtained from the Daymet website (https://daymet.ornl.gov), obtained and distributed by the Oak Ridge National Laboratory Distributed Active Archive Center (ORNL DAAC), one of NASA's data

distribution and archive centers. The data are provided in a 1km x 1km grid of daily weather estimates and are generated using a network of ground observation sites to provide input data which is then processed using the Daymet model algorithm (https://daymet.ornl.gov/overview.html). The algorithm processes the input data, subsetting the data into 2^{o} x 2^{o} tiles which are then processed separately. The data are interpolated by an estimation of station density using a Gaussian filter; the search radius of stations changes depending on the concentration level of stations with more dense areas having a smaller search radius than less dense areas. The model then produces output data [minimum temperature (Tmin, ^{o}C), maximum temperature (Tmax, ^{o}C), incoming shortwave radiation (Rg, J m^{-2} d^{-1}), vapor pressure (P, kPa), snow-water equivalent (kg m^{2}), precipitation (mm), and day length (s)] in continuous raster form for the entire continental United States. Data for the respective years of the selected AmeriFlux study sites (referred to as "field years") were extracted for the various sites under study by using the "Single Pixel Extraction" tool (https://daymet.ornl.gov/dataaccess.html#SinglePixel) with specified latitude, longitude, and date range. Data were then downloaded in CSV format in which average daily temperature, vapor pressure deficit and incoming PAR were calculated in Microsoft Excel. Average daily temperature (T) was calculated as:

$$T = \frac{Tmin+Tmax}{2} \quad (1)$$

Vapor pressure deficit (VPD) was calculated utilizing vapor pressure, P, as:

$$VPD = \frac{0.61078 \cdot e^{(17.269)(T)}}{T+237.8} - P \quad (2)$$

Incoming PAR (µmol m^{-2} d^{-1}) was calculated from incoming shortwave radiation (Rg) as:

$$PARin = Rg \cdot 2.07 \quad (3)$$

The constant 2.07 is computed as the product of 0.45 [since PAR is 45% of total shortwave at the top of the atmosphere (Rg, J $m^{-2}d^{-1}$) (Weiss and Norman, 1985)] and 4.6 [an average 4.6 µmol/Joules over the PAR range] and thus has units of µmol/J.

MODIS Data

Surface reflectance data were obtained from MODIS products MOD09Q1 and MYD09Q1 (Terra and Aqua, respectively) via Google Earth Engine from which the Wide Dynamic Range Vegetation Index (WDRVI) values were calculated; green leaf area index (gLAI) values were determined from the WDRVI time series. The MODIS products are each eight day composite data of surface reflectance (ρ), from MODIS band 1 in the red region (620-670nm, ρ_{red}) and MODIS band 2 in the near infra-red region (841-876nm, ρ_{NIR}) at 250m spatial resolution. Both products provide the best observation per pixel over an eight day period. A WDRVI time series was calculated at eight day intervals as:

$$WDRVI = (\alpha(\rho_{NIR}) - \rho_{red})/(\alpha(\rho_{NIR}) + \rho_{red}) \quad (4)$$

Where α is a weighting parameter; WDRVI is equal to Normalized Difference Vegetation Index (NDVI) when α equals 1, and WRDVI equals zero when α equals (ρ_{red} / ρ_{NIR})

(Gitelson, 2006). Google Earth Engine (https://code.earthengine.google.com) allowed for the quick processing of a time series of WDRVI values, calculated by Google Earth Engine from MODIS data, and downloading for each site over a specified range of time; the range in this case was the respective study dates for each location. The geographic coordinates used to select the pixels for extraction were obtained through the AmeriFlux website (Site Info tab). The WDRVI values from the pixel nearest the geographic center for each field were downloaded and analyzed. Many pixels from the MODIS products not at the geographic center for each field were found to be mixed due to the 250m pixel resolution, with some reflectance coming undoubtedly from non-cultivated areas adjacent to the sites. As an example, US-Br1 inclusion of surrounding pixels resulted in a saw tooth pattern in the WDRVI calculated LAI response curves, indicating the inclusion of vegetated areas in which plant material was removed multiple times throughout the season (mowed or harvested).

Once obtained, WDRVI data were converted to gLAI values. The conversion factors for maize and soybean used in this study are from Nguy-Robertson and Gitelson (2015) and were determined from ground samples at the Nebraska sites:

$$gLAI = (5.06) * (WDRVI\ Value) + (-0.47)\ (Maize) \quad (5)$$

$$gLAI = (3.68) * (WDRVI\ Value) + (-0.24)\ (Soybean) \quad (6)$$

gLAI data were interpolated to continuous daily values for the growing season using Curve Expert 1.4 software (https://www.curveexpert.net/) and a cubic spline interpolation algorithm.

Flux Data

Flux data are provided by the AmeriFlux Network, a system of sites located throughout North and South America and supported by the U.S. Department of Energy. The sites measure carbon, water, and energy fluxes at the field scale using the eddy covariance technique (http://ameriflux.lbl.gov/about/about-ameriflux/). AmeriFlux data were used to calculate daily Gross Primary Production (GPP) values which were then used to both calibrate and validate the model. For field years in which no GPP values were reported, half-hourly (or hourly) averages of GPP were calculated using half-hour (or hourly) averages of net ecosystem exchange (NEE, µmol m^{-2} s^{-1}) and ecosystem respiration (Re, µmol m^{-2} s^{-1}) measurements; NEE was estimated from half-hour (or hourly) averages of canopy carbon dioxide flux (Fc, µmol m^{-2} s^{-1}). NEE values were screened by graphing these values as a function of concurrent AmeriFlux measured half-hour (or hourly) averages of PAR (µmol m^{-2} s^{-1}) and removing obvious outliers. For field years where PAR was not available, it was calculated from incoming solar radiation (Rg, µmol m^{-2} s^{-1}) by dividing Rg by 2, as PAR comprises roughly half of Rg (Weiss and Norman, 1985). Daytime interpolation of NEE and nighttime interpolation of AmeriFlux measured ecosystem respiration (Re, µmol m^{-2} s^{-1}) were then conducted.

Half-hour averages were converted into half hour fluxes by multiplying the averages by 1800 s (half-hour)$^{-1}$; hourly averages were converted to hourly fluxes by multiplying the averages by 3600 s h^{-1}. Daily GPP was determined as the sum of daily NEE [half-hourly NEE fluxes (hourly for Mead sites)] and daily Re [half-hourly Re fluxes (hourly for Mead sites)]:

$$GPP = NEE - Re \quad (7)$$

All units were converted to mg CO_2 µmol^{-1} (by multiplying µmol m^{-2} s^{-1} by 44 µg CO_2 µmol^{-1} *1000 mg µg^{-1}). Note the sign convention is that fluxes towards the surface (i.e., GPP) are positive and fluxes away from the surface (i.e., Re) are negative. Daily GPP values were integrated from hourly average CO_2 (mg C m^{-2} s^{-1}) to daily units of C (g C m^{-2} d^{-1}) for all sites. CO_2 was converted to C by multiplying GPP by 12 g C mol^{-1}/44 g CO2 mol^{-1} (carbon has an atomic mass of 12 while oxygen has an atomic mass of 16). The fluxes are reported as positive when the direction of the flux is towards the earth's surface and are likewise reported as negative when their direction is away from the earth's surface. Field year growing season start and end dates were determined using GPP data; start dates were determined to be days in which GPP values commenced to be greater than zero and end dates were determined to be days in which GPP values fell below the zero threshold.

Light Use Efficiency Model

A simple light use efficiency model is used to estimate GPP (Monteith, 1972). The model has been adapted by Nguy-Robertson et al. (2015) to incorporate scalars taken from other GPP models. The four scalar light use efficiency modeling approach of Nguy-Roberson et al. (2015) hereto referred to as the light use Efficiency GPP Model (EGM) was used in estimating GPP where:

$$GPP = \varepsilon_0 \times C_{scalar} \times T_{scalar} \times W_{scalar} \times P_{scalar} \times APAR \quad (8)$$

ε_0 is the daily light use efficiency during clear sky conditions, APAR is the absorbed photosynthetically active radiation, and the scalars account for impact of diffuse light (C_{scalar}), air temperature (T_{scalar}), water stress (W_{scalar}), and phenology (P_{scalar}). ε_0 and the four scalars combined represent the well-known daily light use efficiency term, ε of Monteith (1972):

$$GPP = \varepsilon \, x \, APAR \quad (9)$$

The calculations of the scalars in this study follow that of Nguy-Robertson et al. (2015) but instead of AmeriFlux on-site meteorological and biophysical observations as model input, gridded Daymet and MODIS derived LAI values were used. A summary is provided here but the reader is directed to the Nguy-Robertson et al. (2015) paper for details (see Appendix).

- C_{scalar} accounts for the effects of diffuse lighting on photosynthesis (Suyker and Verma, 2012),

- T_{scalar} accounts for the effects of daytime air temperatures (Raich et al. 1991; Kalfas et al. 2011),
- W_{scalar} accounts for water stress effects (Wu et al, 2008; Maselli et al. 2009),
- P_{scalar} incorporates phenology effects (Kalfas et al, 2011; Wang et al, 2012), and

$$APAR = PARin\ x\ (1 - e^{-k \times gLAI}) \quad (10)$$

Where gLAI is the leaf area of the canopy engaged in photosynthesis and *k* is the light extinction coefficient.

C_{scalar} accounts for the effects of diffuse lighting on photosynthesis (Suyker and Verma, 2012). Plants tend to use diffuse light more efficiently than direct sunlight on overcast days where lighting is more diffuse than on clear days, penetrating the canopy more effectively, so that Ɛ will increase. C_{scalar} is calculated as:

$$Cscalar = 1 + \beta \times ((\frac{PARd}{PARin}) - 0.17) \quad (11)$$

The term β is the sensitivity of the daily light use efficiency to diffuse light and PARd is the diffused PAR. On days in which there is a negligible amount of diffuse light, the quotient of terms PARd and PARin is equal to 0.17. The term -0.17 ensures the terms sum to zero when diffuse light is insignificant (i.e., when the quotient of terms PARd and PARin is equal to 0.17). PARd is approximated using the approach outlined by Nguy-Robertson et al. (2015) using a cloudiness coefficient (CC) term which is determined using PARin and PAR potential:

$$CC = 1 - \left(\frac{PARin}{PARpot}\right) \quad (12)$$

PAR_{pot} refers to the estimated potential amount of incoming photosynthetically active radiation, accounting for influences such as time of year, latitude, atmospheric pressure and elevation (according to Weiss and Norman, 1985, with corrections in Nguy-Robertson et al., 2015).

T_{scalar}, initially developed by Raich et al. (1991), takes into account temperature effects on photosynthesis and is calculated using Eq. 8 and the given constants in Nguy-Robertson et al. (2015). The weather input from Daymet for this variable is the mean daily temperature, T, calculated as the average of the Daymet minimum and maximum temperatures. T_{min}, T_{max}, and T_{opt}, are constants first identified by Kalfas et al. (2011) as 10, 48, and 28 ^{o}C respectively:

$$T_{scalar} = \frac{(T - 10) \times (T - 48)}{[(T - 10) \times (T - 48)] - (T - 28)^2} \quad (13)$$

W_{scalar} accounts for water stress effects on photosynthesis and was calculated based on VPD using Eq. 2 and associated constants in Nguy-Robertson et al. (2015). Nguy-Robertson et al. (2015) modeled this scalar by synthesizing the approach of Wu et al. (2008) and Maselli et al. (2009), as water stress can be introduced both through atmospheric water deficits and soil water deficits. Unlike models in which the scalar remains constant until a critical threshold for VPD is reached, the EGM utilizes no threshold for VPD and the scalar was allowed to vary based on the Daymet data.

σW_{scalar} is a term for the curvature parameter for water stress as proposed by Gilmanov et al. (2013) to account for varying convexity for the relationship between photosynthesis and water stress:

$$W_{scalar} = exp\ \{ - [\ (VPD/\sigma W_{scalar})^{2}\ ]\ \} \quad (14)$$

P_{scalar} accounts for leaf phenology, as leaves that are immature do not photosynthesize as efficiently as mature leaves, and leaves that are senescing do not have an optimal photosynthetic capacity (Reich et al. 1991; Field and Mooney 1983). The scalar is calculated using green leaf area index (gLAI), maximum gLAI (gLAImax), a constant maximum LAI value that is specific to each crop (as defined in Nguy-Robertson et al., 2015); σP_{scalar} which is the curvature parameter for relationship between photosynthesis and phenology:

$$P_{scalar} = exp\{ - [\ ((gLAImax - gLAI)\ /\ (\ \sigma P_{scalar}\ ))^{2}\ ]\ \} \quad (15)$$

Calibration and Validation

Four basic steps were followed in this study:

1) Select field years for model calibration; remaining field years will be used for validation.
2) Calibrate the EGM by establishing scalars using AmeriFlux cropland sites for selected years and satellite derived input and gridded weather datasets;
3) Apply the EGM with estimated scalars (from step 2), satellite data and gridded weather data sets for the field years held for validation;

4) Evaluate the EGM estimated daily GPP to AmeriFlux observed daily GPP

1. Data Selection;

To run the EGM, several coefficients were calculated from the Daymet and MODIS derived gLAI data using an R script (A. Nguy-Robertson, personal communication, 2015). For statistical purposes, a certain number of field years were chosen randomly to calibrate the model (i.e., to obtain the EGM scalar coefficients); the remaining field years were used for "validation." Field years for calibration were sampled randomly without replacement using a random number generator in Microsoft Excel. First, each geographic location (Mead, Bondville, Brooksfield, and Rosemont) was assigned a number and was chosen at random using the random number generator. From there, each site at the location (for locations that contain multiple sites) was assigned a number and was selected at random using the random number generator. Once the site was selected, approximately 75% of the field years for the site for a particular crop were randomly selected for calibration, while ensuring that at least one field year for each crop type was reserved for validation purposes. This process was repeated until the desired number of calibration and validation field years for each site and crop was fulfilled (Tables 2 and 3).

Table 2: Ameriflux calibration field years

Calibration Years		
Site	**Maize**	**Soybean**
US-Ne1 (NE - irrigated)	2002-2005, 2007, 2009-2012	--
US-Ne2 (NE - irrigated)	2003, 2005, 2007, 2009,2013	2002, 2004, 2008
US-Ne3 (NE)	2003, 2005, 2011, 2013	2006, 2008, 2010, 2012
US-Br1 (IA)	2005, 2007, 2009	2006,2008
US-Br3 (IA)	2006, 2010	2007, 2009, 2011
US-Bo1 (IL)	2001, 2005, 2007	2002, 2004
US-Ro1 (MN)	2005, 2009, 2011	2006, 2010, 2012
Field Years	**29**	**17**

Table 3: Ameriflux validation field years

Validation Years		
Site	**Maize**	**Soybean**
US-Ne1 (NE - irrigated)	2006, 2008, 2013	N/A
US-Ne2 (NE - irrigated)	2011,2012	2006
US-Ne3 (NE)	2007, 2009	2002, 2004
US-Br1 (IA)	2011	2010
US-Br3 (IA)	2008	2005
US-Bo1 (IL)	2003	2006
US-Ro1 (MN)	2007	2008
Field Years	**11**	**7**

2. Calibrate the EGM by establishing scalars using AmeriFlux cropland sites for selected years and satellite derived input and gridded weather datasets;

Selected field year flux data, Daymet derived (Tavg, VPD, CC, APAR and T_{scalar}) and remotely-derived gLAI were used to derive $\varepsilon_{0,}$ β and CC (for the C_{scalar}), T_{scalar}, σW_{scalar} and VPD (for the W_{scalar}), and σP_{scalar} (for the P_{scalar}) values. These data were input into an R script that, through an iterative training process as described in Nguy-Robertson et al. (2015) (see Appendix), determined separate parameters for irrigated and non-irrigated maize and soybean crops. The script trained the parameters using a step-by-step method in which each scalar was estimated one at a time. During the iteration in which a parameter is calculated, assumptions are made about the other parameters to mimic optimal field conditions. Once the parameters are calculated the iterations are repeated using the entire calibration dataset to include the calculated parameters, AmeriFlux derived GPP, Daymet derived Tavg, VPD, CC, APAR and T_{scalar}, and remotely derived gLAI data. Output from the R script for both maize and soybean were $\varepsilon_{0,}$ β, σW_{scalar}, and σP_{scalar} values along with the corresponding standard deviation for each. Additionally, $gLAI_{max}$ values for both irrigated and rainfed soybean and maize were calculated in Microsoft Excel from MODIS derived gLAI data. From these outputs, scalars were calculated through an Excel template that utilized Eqs. 8-15.

3. Apply the EGM with estimated scalars (from step 2), satellite data and gridded weather data sets to independent data from cropland sites;

The validation data left out from the calibration step for each site along with the calibrated scalars were used in the EGM to estimate GPP for validation years.

4. Evaluate the estimated daily GPP to AmeriFlux observed daily GPP

The estimated GPP were compared to the observed AmeriFlux determined GPP using linear regression and the root mean squared error (RMSE) index (Willmott, 1981),:

$$RMSE = \sqrt{N^{-1}\sum_{i=1}^{N}(M_i - O_i)^2} \quad (16)$$

where M is modeled GPP and O is observed or measured GPP. RMSE was calculated as a way to quantify the magnitude of the error in the model which could be concealed by opposing high and low residuals in a simple linear regression where R^2 is reported. Additionally, mean normalized bias (MNB) was calculated to provide a unitless measure of model error to allow for cross-species comparisons between maize and soybean (Yu et al., http://www.ecd.bnl.gov/steve/pres/metrics.pdf):

$$MNB = \frac{1}{N}\sum_{i=1}^{N}\left(\frac{M_i - O_i}{O_i}\right) x\ 100\% \quad (17)$$

Where M is the modeled (EGM) GPP and O is the measured (Ameriflux) value.

CHAPTER 3 RESULTS AND DISCUSSION

For each site, field years for a particular crop were randomly selected for calibration and the process repeated; 46 out of the 65 total field years were designated as calibration field years while 19 out of 65 were designated as validation field years (resulting in 71% of field years used for calibration and 29% used for validation) (Tables 2 and 3). Crop type, daily GPP (from AmeriFlux), T, VPD, APAR, CC, and T_{scalar} (derived from Daymet gridded data using Eqs. 1, 2, 10, 12, and 13, respectively), and gLAI (derived from MODIS data from Eqs. 5 and 6) for the calibration field years were then read in to the R script iterative process along with constants from Nguy-Robertson et al. (2015) to estimate the parameters ε_0, β, σW_{scalar}, σP_{scalar}, and $gLAI_{max}$ to represent the selected AmeriFlux sites and crops in the EGM. These parameters, used to drive the EGM, differed slightly from those reported in Nguy-Robertson et al. (2015) (Table 4). In using field years from more climatically diverse locations in the calibration process, the parameters were generalized to best fit conditions across all study locations of the northern Midwest region (and not just southeastern Nebraska as in the Nguy-Robertson et al. (2015) study). The parameters ε_o, β, $\sigma_{Pscalar}$ and $gLAI_{max}$ differed from those of Nguy-Robertson et al. (2015) while $\sigma_{Wscalar}$ was the same. The constants k, T_{min}, T_{max}, and T_{opt}, were the same as those used by Nguy-Robertson (2015) study. Data from the

Table 4: Parameters for the calculation of scalars for EGM model. The parameters at the top were calculated through the iterative R script process while the parameters at the bottom are model constants.

				Nguy-Robertson et al. 2015		This study	
Variables	**Symbol**	**Eqs**	**Units**	**Maize**	**Soybean**	**Maize**	**Soybean**
Derived through iterative process:							
Maximal light use efficiency	ε_0	(8)	g C mol^{-1}	0.526±0.007	0.374±0.005	**0.573±0.002**	**0.407±0.002**
Sensitivity of ε to diffuse light	β	(11)	Unitless	0.347±0.051	0.411±0.056	**0.181±0.014**	**0.294±0.020**
Water stress curvature parameter	σW_{scalar}	(14)	kPa	6±0.25	4±0	**6±0**	**4±0**
Phenology curvature parameter	σP_{scalar}	(15)	$m^2\ m^{-2}$	18±4.59	18±7.15	**7±0**	**8±0**
Calculated in Excel:							
Maximal green leaf area index [irrigated]	$gLAI_{max}$	(10), (15)	$m^2\ m^{-2}$	4.93[6.78]	4.63[6.15]	**5.04[5.14]**	**3.86[4.25]**
Constants							
Light extinction coefficient	k	(10)	Unitless	0.443	0.601	**0.443**	**0.601**
Minimum temperature for physiological activity	T_{min}	(1), (13)	°C	10	10	**10**	**10**
Maximum temperature for physiological activity	T_{max}	(1), (13)	°C	48	48	**48**	**48**
Optimal temperature for physiological activity	T_{opt}	(13)	°C	28	28	**28**	**28**

validation field year datasets (Tables 2 and 3) and parameters derived from the iterative process (Table 4) along with specified constants were used to calculate daily values of the scalars, C_{scalar}, W_{scalar}, and P_{scalar} (Eqs. 11, 14, and 15) and APAR (Eq. 10) from which daily GPP values were estimated (Eq. 8).

Estimated daily GPP for maize and soybean for the selected validation field years were compared to observed AmeriFlux determined daily GPP and indicate a strong correlation (R^2 = 0.80) and an overall RMSE of 3.5 g C $m^{-2}d^{-1}$ (Fig. 1a). However, the (MNB) was 30.5%. The RMSE for overall maize field years was 3.7 g C $m^{-2}d^{-1}$, the R^2 was 0.82, and the MNB was 17.9% (Fig. 1b) while the RMSE for overall soybean field years was 3.2 g C $m^{-2}d^{-1}$ with an R^2 of 0.64 and a MNB of 53.6% (Fig. 1c). The lower RMSE for soybeans is attributed to soybeans having approximately 30% lower GPP than maize. Despite the lower RMSE, the model performed less effectively with soybean as soybean RMSE is only 14% lower than maize RMSE while soybean GPP was 30% less than maize. In a measure of cumulative bias, growing season GPP modeled values agree with measured growing season GPP values with an RMSE of 126 g C m^{-2} y^{-1}, an R^2 of 0.9, and MNB of 4.5% (Fig. 2).

Two trends are apparent from the comparison graphs for each crop and site. One is that, for soybean crops, the model tends to overestimate GPP when daily GPP values are higher and, for both maize and soybean crops, the model tends to underestimate when GPP values are very low (Figs. 3 and 4). Model underestimation at

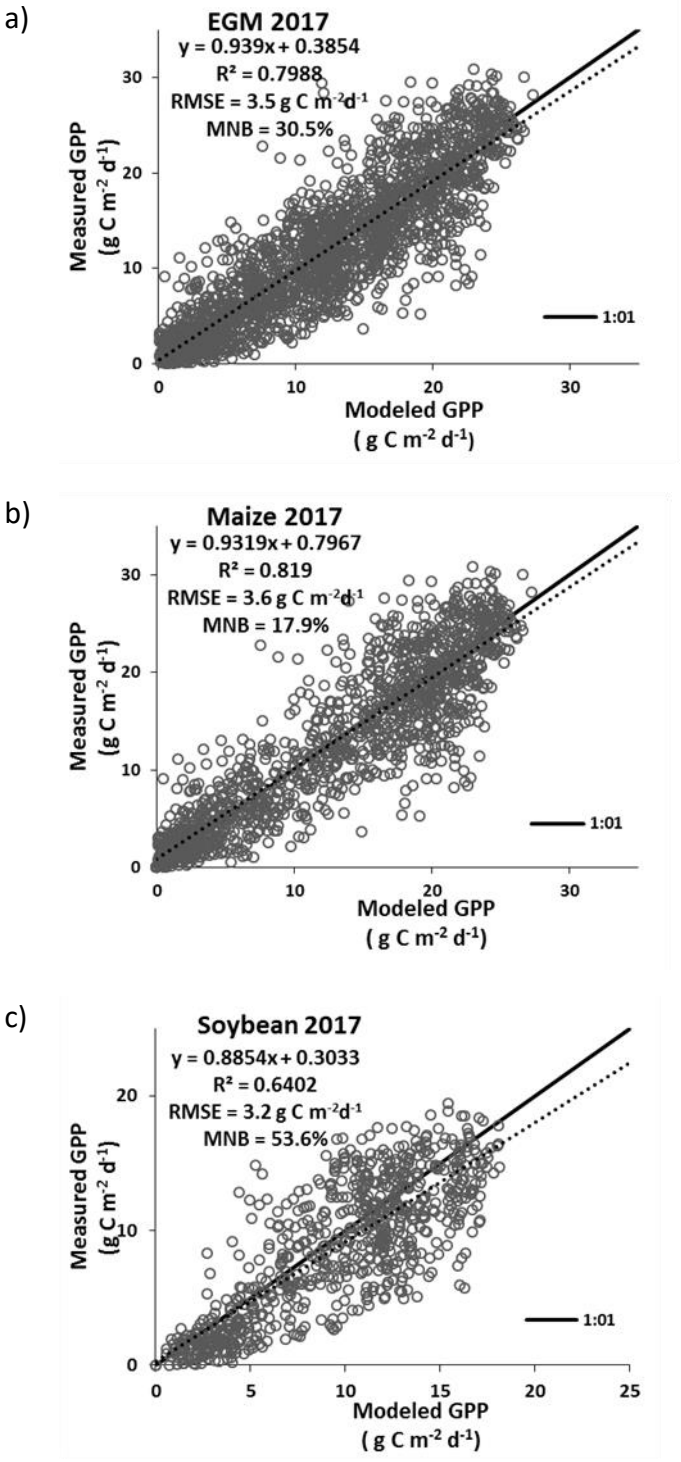

Figure 1: The relationship between AmeriFlux measured and EGM modeled GPP for a) all validation data, b) all maize validation data, and c) all soybean validation data.

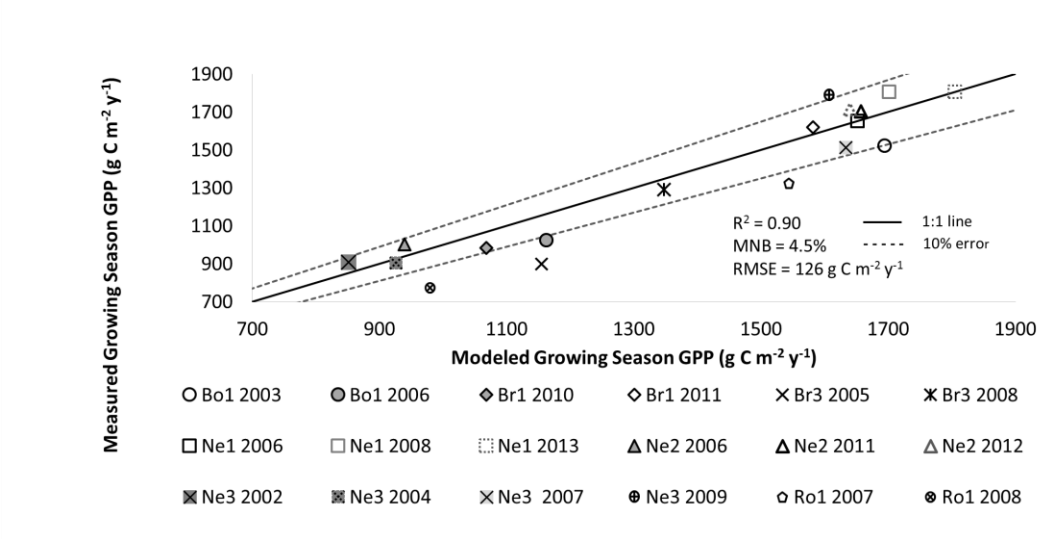

Figure 2: AmeriFlux measured GPP yearly total vs EGM modeled GPP yearly totals for every validation field year.

low GPP could be due to the insensitivity of the MODIS sensors to low levels of biomass. The other trend is that the strength of the correlation between measured and modeled GPP values is stronger with the maize than with the soybean datasets (R^2 of 0.69 to 0.89 for maize and 0.55 to 0.75 for soybeans). The increased sensitivity to diffuse light of soybean plants when compared to maize (β of 0.294 ± 0.002 for soy, 0.181 ± 0.014 for maize) combined with the concerns regarding PARin data (discussed below) may partially explain the poorer estimates. Estimates of soybean gLAI may be a factor as well since the gLAI algorithm for soybean was developed for the Mead, NE training sites (US-Ne2 and US-Ne3) and may not adequately estimate gLAI for the other locations that may have varying planting densities. The Mead sites have lower RMSE and higher correlation between measured and modeled GPP than the other soybean sites (Table 5).

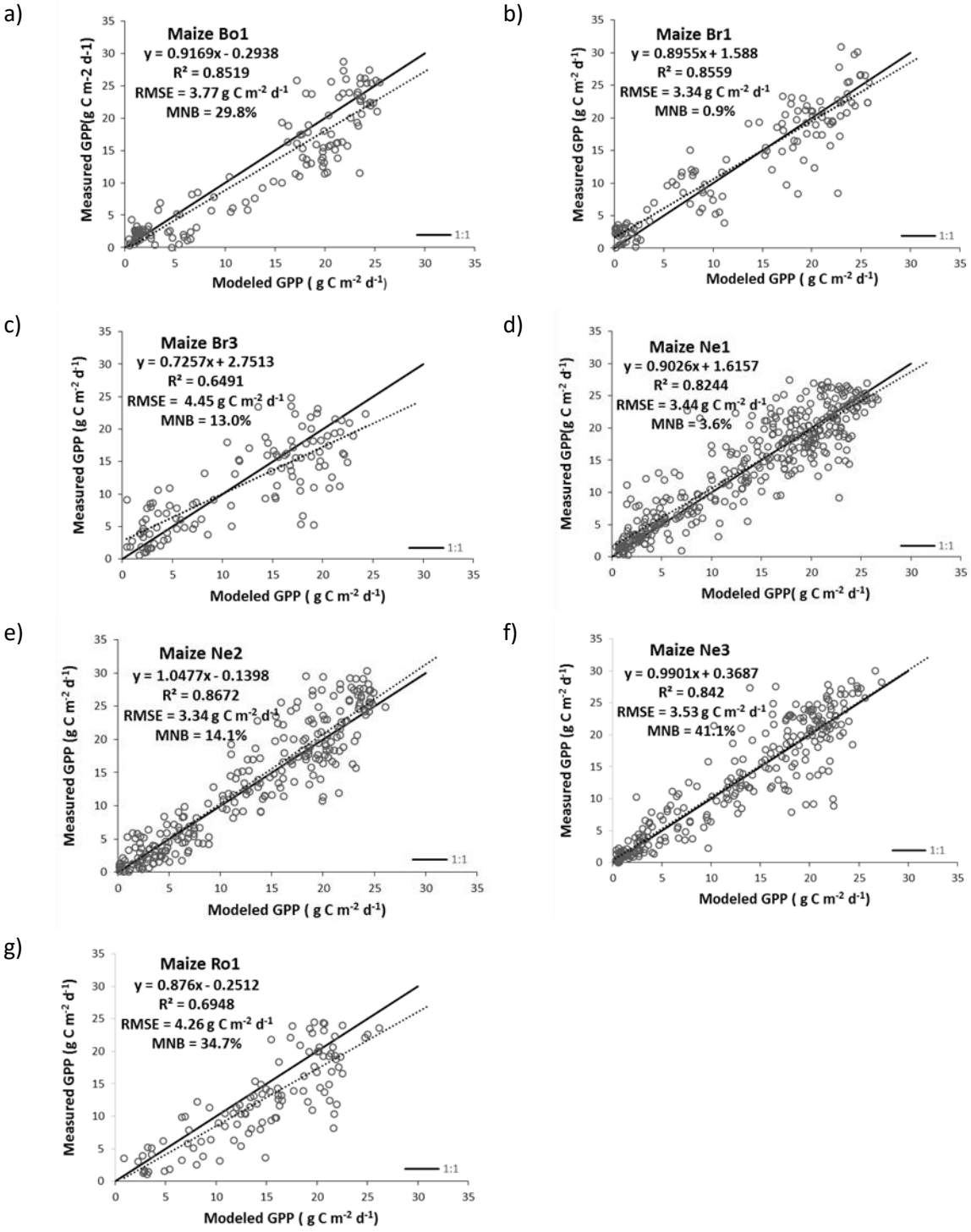

Figure 3: Measured AmeriFlux vs modeled EGM GPP for all maize validation years by site.

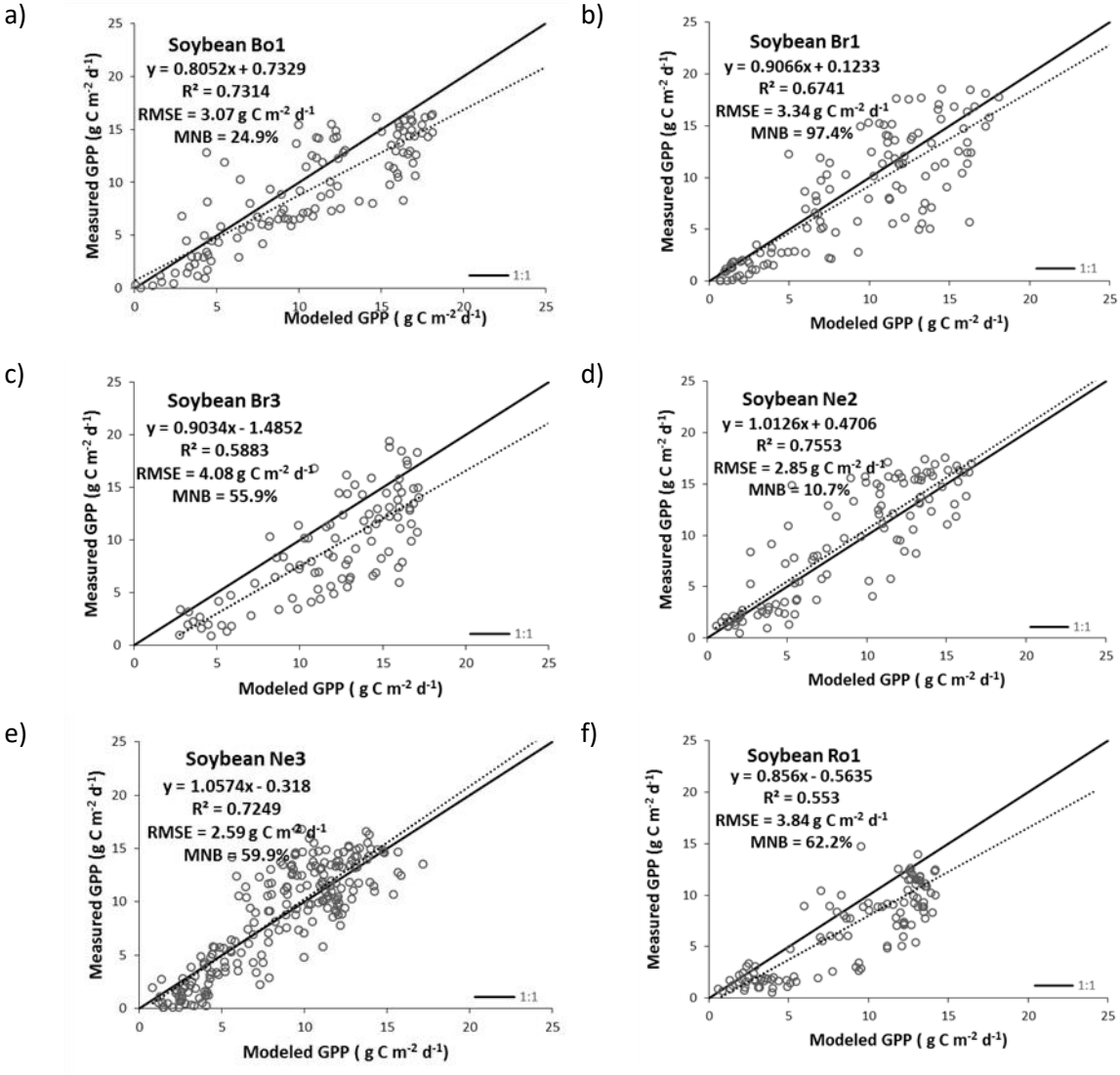

Figure 4: Measured AmeriFlux vs modeled EGM GPP for all soybean validation years by site.

Additionally, there were fewer soybean field years (17) than maize field years (29) with which to train the scalars which may have allowed for more error in the soybean scalars due to the smaller sample size (Table 2).

Table 4: RMSE values for the comparison of modeled daily GPP values to observed daily GPP values for each AmeriFlux research site in the study. The top row indicates the total error for the site while the second and third rows indicate error for maize and soybean, respectively. The final column totals error overall and by crop type.

	Daily GPP RMSE (g C m^{-2} d^{-1})							
	US-Bo1	**US-Br1**	**US-Br3**	**US-Ne1**	**US-Ne2**	**US-Ne3**	**US-Ro1**	**All**
Total	3.47	3.34	4.29	3.44	3.21	3.14	4.05	3.51
Maize	3.77	3.34	4.45	3.44	3.34	3.53	4.26	3.65
Soybean	3.07	3.34	4.08	N/A	2.85	2.59	3.84	3.20

The agreement is not as strong as that between modeled maize and soybean GPP reported by Nguy-Robertson et al. (2015) with an overall R^2 value of 0.91 and an RMSE of 2.6 g C m^{-2} d^{-1}; the MNB for this study was 1.7%, thus, the MNB of 30.5% for the current study is of concern. It was expected that error would increase when using modeled input data as opposed to measured input data specific for the site (as was the case for Cui et al., 2016, who attained an RMSE of 2.973 g C $m^{-2}d^{-1}$ when comparing their modeled GPP data to *in situ* derived GPP of mixed land cover in the Heihe River Basin, China). There are inherent errors and uncertainties in the gridded Daymet data (Mourtzinis et al., 2016) which are attributed to the weaker agreement between measured and modeled daily GPP values. In addition, the LAI algorithms used in this study were developed using the Mead sites (Nguy-Robertson and Gitlson, 2015) and may not be ideal estimators of the LAI for the other sites as the red band is known to be insensitive to high biomass, regardless of crop type (Nguy-Robertson and Gitelson, 2015).

Comparison of Daymet derived values to those measured at the AmeriFlux sites demonstrated T_{ave} values did not have a data quality issue as did PARin and VPD (Fig. 5). T_{ave} values (Eq. 1, using Daymet T_{min} and T_{max}) had an R^2 value of 0.95, an RMSE of 2.4°C, and a MNB of 2.98% when compared to AmeriFlux measurements (Fig. 5a) while daily PARin values had an R^2 value of 0.48, an RMSE of 30.5 $mol^{-1}d^{-1}$, and a MNB of 57.9% when compared to AmeriFlux measured PARin values (Fig. 5b), and VPD (Eq. 2 using Daymet vapor pressure) comparison to measured values had an R^2 value of 0.54, an RMSE of 0.31 kPa, and a MNB of 98.3% (Fig. 5c).

In their study, Mourtzinis et al. (2016) calculated an R^2 value of 0.24 for Daymet incoming shortwave radiation, an R^2 value of 0.48 for relative humidity (calculated from vapor pressure), an R^2 value of 0.94 for T_{min}, and an R^2 value of 0.92 for T_{max} when modeled Daymet data were compared to measured weather data retrieved from MESONET weather network stations (http://mrcc.isws.illinois.edu/gismaps/mesonets.htm). Since the daily temperature products from Daymet are derived from interpolated ground station measurements, it is not surprising to find a strong correlation between their values and the values obtained from the AmeriFlux network. Mourtzinis et al. (2016) also conclude good levels of accuracy in modeled Daymet minimum and maximum temperature values. Since vapor pressure and incoming shortwave are modeled, however, these products have a much weaker correlation to the measured AmeriFlux data (Fig. 5).

a)

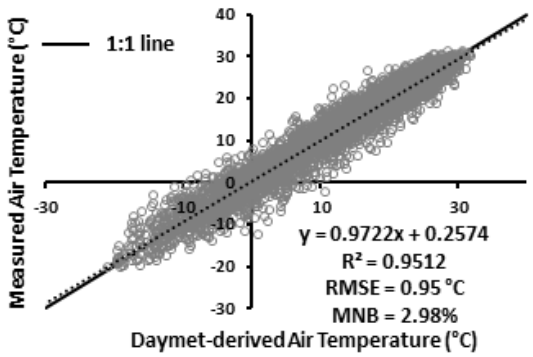

b)

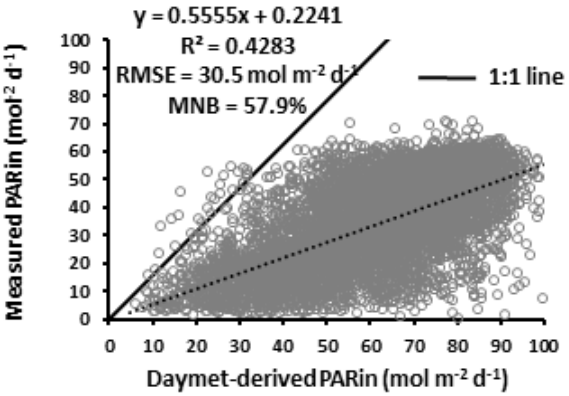

c)

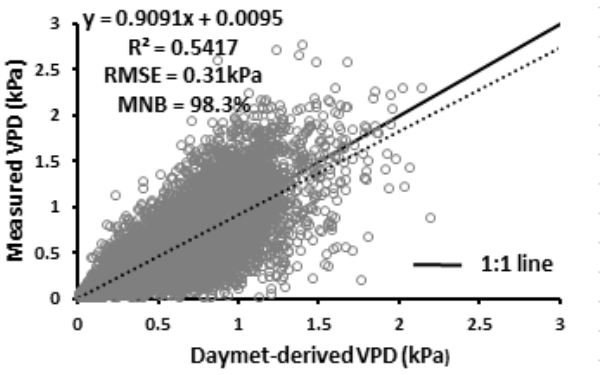

Figure 5: AmeriFlux measured values as functions of estimated Dayment daily values for: a) average daily temperature, b) PARin and c) VPD.

The Daymet model calculates incoming shortwave radiation, Rg, (from which PARin is estimated) using sun-slope geometry based on time of year and location on Earth (https://daymet.ornl.gov/overview.html). The model does not take into account the many local weather factors and local aerosol variability that can affect the amount of shortwave radiation that reaches the ground, therefore on days in which weather conditions hinder the penetration of incoming shortwave radiation the model will overestimate the product. Mourtzinis et al. (2016) attributed the model to poor estimates of Rg. Additionally, studies conducted using other sources of modeled incoming shortwave have found similar trends in overestimation of the data (e.g. Liu 1997; Matsushita and Tamura 2002); in the Matsushita and Tamura (2002) study, the data were corrected using a reduction coefficient of 0.63. Likewise, in the Liu (1997) study, incoming shortwave radiation was corrected using a reduction coefficient of 0.62. The Daymet model estimates vapor pressure (which is used to calculate VPD for this study) using an algorithm that produces vapor pressure values as a function of minimum daily temperature and average daily daylight temperature. Mourtzinis et al. (2016) likewise attributed the method the Daymet model uses to the poor estimates, stating that there are uncertainties in the way vapor pressure is estimated from T_{min} and T_{max}.

The trend in this study for an overestimation of PARin (Fig. 5b) would result in a trend for a decrease in the C_{scalar} value and should be self-corrected in the calibration. This suggests an unsystematic bias in the PARin (and thus APAR) and brings to question

the Daymet models used to calculate shortwave radiation (which PARin is estimated from). An overestimation of PARin reduces the model's ability to properly account for the contributions of diffuse light to GPP and, thus, would inaccurately lower the modeled GPP. The overestimation of VPD by Daymet likely is due to the air mass over agricultural fields, especially irrigated agricultural fields, having lower VPD than what is reported within the grid the fields are located. The overestimation of VPD decreases the W_{scalar} value which causes the model to not always represent water stress conditions at the sites. Additionally, the calibration is influenced by the two irrigated Mead sites (US-Ne1 and US-Ne2) which may have biased the σW_{scalar} parameter to better reflect irrigated crop management practices while the other five fields are under rainfed crop management. A direct comparison of W_{scalar} values calculated from Daymet data against W_{scalar} values calculated from AmeriFlux data at the three Nebraska sites shows an R^2 of 0.51, indicating that the poor quality VPD data from Daymet likely had an effect on the scalar and minimized the benefit of including such a scalar (Fig 6). Although the scalars may not have been as effective as they could have been if more accurate input data were available, overall the model performed better with the scalars derived in this study using the Daymet and MODIS data than it did when run as strictly a LUE model. For comparison purposes the EGM was run with all scalars set to a value of 1 so as not to have any effect on the GPP calculation. GPP calculated with the scalars set to 1 had an RMSE of 5.35 g C m^{-2} d^{-1}, an R^2 of 0.72, and a MNB value of 103.44% (Fig. 7).

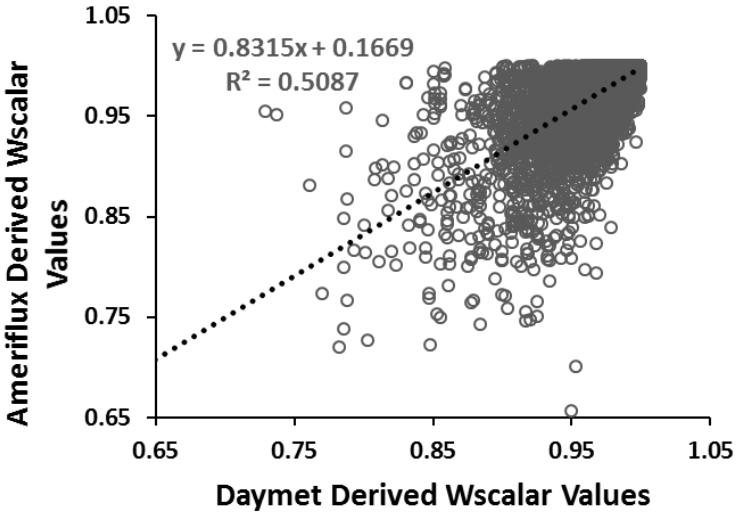

Figure 6: AmeriFlux derived W_{scalar} values (unitless) plotted as a function of Daymet derived W_{scalar} values for US-Ne1, US-Ne2, and US-Ne3 validation years. The maximum value for the scalar is 1 and the value is downgraded as water-stress conditions increase.

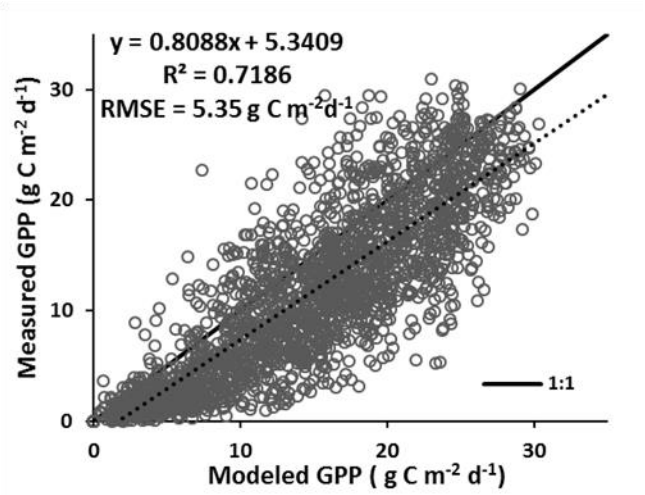

Figure 7: AmeriFlux measured GPP plotted as a function of EGM modeled GPP when all scalar values are set to 1. In this configuration, the model is run as a pure LUE model with the scalars completely negated.

Suyker and Verma (2012) showed through isolating PAR and LAI as variables for GPP modeling that PAR was one of the predominant factors in GPP variability. Additionally, Hazarika et al. (2004) concluded that LAI is the primary determinant of

productivity using their model (Sim-CYCLE) to estimate net primary productivity. Thus, PARin and gLAI values (which also affect APAR values) likely are the main contributors to the scatter about the 1:1 line and the high MNB. An overestimation of PARin greatly affects APAR in a manner that causes an overestimation of GPP and, as there is more weight assigned to the APAR variable than the scalars, the result is an overall overestimation of GPP when PARin is overestimated. This overestimation will inflate the MNB. Estimated APAR (Eq. 10) for the three Nebraska sites was plotted as a function of measured APAR in an attempt to determine how well the model was estimating the variable. Two of the inputs in calculating APAR are gLAI and PARin, and a good portion of the increased error is attributed to this term in the GPP equation (Eq. 8). When compared to measured APAR, estimated APAR for the three Nebraska sites (US-Ne1, US-Ne2, and US-Ne3) had a combined RMSE of 10.8 $m^2\ d^{-1}$ and an R^2 of 0.53 (Fig 8a). When the data are separated into green-up (DOY ≤ 220) and post-green peak (DOY > 220) sets, it becomes apparent that there is a stronger correlation between measured and modeled APAR during the green-up phase than the post green-up phase. Measured vs modeled APAR at all Nebraska sites are show a green-up RMSE of 9.0 Mol $m^2\ d^{-1}$ and an R^2 of 0.7 while the post green peak RMSE is 12.7 Mol $m^2\ d^{-1}$ and the R^2 is 0.33 (Figs 8b and 8c). The data show that APAR is estimated more accurately by the model before green peak is reached and that post-green peak APAR data are contributing error to the model.

a)

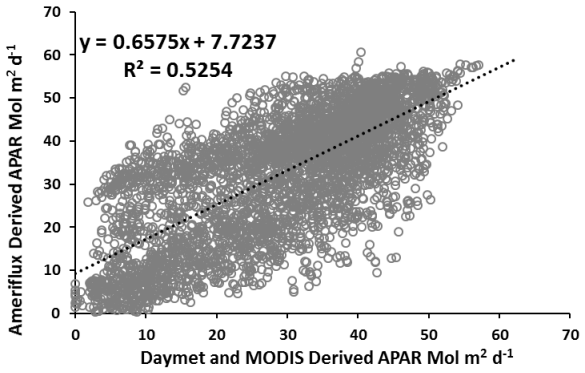

b)

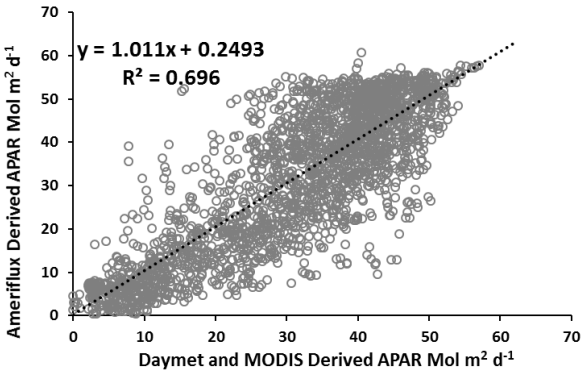

c)

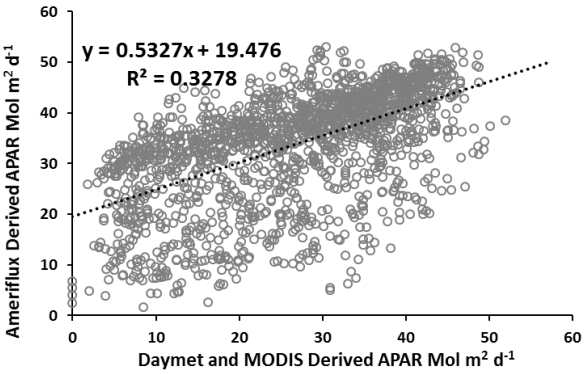

Figure 8: AmeriFlux derived APAR as a function of Daymet and MODIS derived APAR for: a) all growing season days for all three Nebraska sites, b) all green-up days for all three Nebraska sites, c) all post green peak days for all three Nebraska sites.

This study utilized seven fields from four separate geographic locations. However, three of the seven fields, which include 36 of the 65 total field years, are located in southeastern Nebraska, which may have contributed to a calibration bias. This bias may have led to lower error being reported for the Nebraska sites and to a higher error being reported for the non-Nebraska sites than would have otherwise been the case if the field years were more evenly represented for model calibration (Table 2). When comparing the results of this study to the previous Nguy-Robertson et al. (2015) study, some of the increase in error experienced in this study could be explained by the inclusion of four sites not utilized in the Nguy-Robertson study. Since the Nguy-Robertson modeled GPP for only three fields located within a couple of miles from one another, there is less climatic variation in the data to cause inaccuracies in the model. Not only does the addition of more sites in itself add variation to the data, the addition of more sites located hundreds of miles from one another add a considerable amount of climatic variation. Additionally, the inclusion of more field years in general also certainly contributed to increased error for this study. Inherently then, larger error was expected from this new study of the EGM and larger error was indeed observed. However, the effectiveness of the model in estimating daily GPP at four separate geographical locations in the upper Midwest may counterbalance this increased error for researchers interested in modeling GPP at a broader, regional scale. For such researchers, the EGM provides an improved remote sensing daily GPP model over a simple LUE model (Figs. 1a

and 7), and the EGM's accuracy will increase as more accurate gridded weather data are developed.

CHAPTER 4 SUMMARY AND CONCLUSIONS

By incorporating MODIS imagery and Daymet weather data into the EGM used by Nguy-Robertson et al. (2015), daily GPP estimates were derived over seven sites in four upper-Midwestern locations. Overall RMSE between measured GPP and modeled GPP for all field years was found to be 3.5 g C $m^{-2}d^{-1}$. While this is an increase in RMSE of 0.9 g C $m^{-2}d^{-1}$ when compared to Nguy-Robertson et al. (2015), this study incorporates sites geographically separated within the northern Midwest region. Of concern was the MNB of 30.5% for this study. Through calibrating the model with remotely sensed gLAI data and modeled weather data from all seven sites, a set of generalized scalars were developed that functioned for maize and soybeans at each site. However, GPP estimation was better at some sites than others, especially at the Mead sites. Although the accuracy of the EGM was reduced when utilizing remotely sensed and gridded weather data inputs, the difference in accuracy was offset by the reduction in resources required as such inputs negate the need for *in situ* data. While this study indicates that the parameters of the Nguy-Robertson et al. (2015) EGM can estimate GPP that has promising correlation to measured GPP for regions outside merely eastern Nebraska, future research could be conducted to determine if more generalized coefficients can be derived to allow the model to function accurately at broader regional scales

The overestimation of modeled PARin and VPD accuracy issues in the Daymet data may have led directly to an overestimation in GPP which could account for much of

the increase in error between this study and the Nguy-Robertson et al. (2015) study. In particular, the inclusion of 17 irrigated field years from US-Ne1 and US-Ne2 may have biased σW_{scalar}, the curvature parameter for water stress, which would increase error in modeled GPP at the other five study sites. The VPD overestimation at the two irrigated sites, due to the VPD at the sites being anthropogenically lowered through the irrigation practice, would have contributed to this process. Further studies should focus on reducing this error by obtaining more accurate modeled weather inputs.

Since Daymet incoming shortwave (from which PARin was estimated) tends to be overestimated, future researchers may attempt to predict and minimize error related to this overestimation as in the Matsushita and Tamura (2002) study. Likely, other sources of PARin are needed (e.g., Nasahara, 2009; Sakamoto et al., 2011). Likewise, due to the poor quality of the Daymet vapor pressure product, and due to the fact that the vapor pressure product is not inaccurate in as predictable a manner as incoming shortwave, a new source for this variable may need to be found. One such source for both VPD and PARin data could be PRISM (Parameter-elevation Relationships on Independent Slopes Model; PRISM Climate Group (2004)), which was found by Mourtzinis et al. (2016) to be more accurate than Daymet, though it does still have accuracy issues of its own.

Additionally, the gLAI algorithms utilized in the model were developed from a previous study (Nguy-Robertson and Gitelson, 2015) which used the same three Nebraska sites used in this study. While the algorithms were able to derive a gLAI

estimate that correlates to measured gLAI estimates at the other study locations, gLAI estimations were not confirmed with measured values at these sites. Due to lack of *in situ* gLAI data for these sites, a direct comparison was not possible. Of concern is the relationship with the gLAI after peak green up. When adapting this model to provide regional estimates of GPP, future researches should focus on developing and confirming generalized, regional gLAI algorithms for maize and soybean.

REFERENCES

Beer, C., Reichstein, M., Tomelleri, E., Ciais, P., Jung, M., Carvalhais, N., Rodenbeck, C., Arian, M., Baldocci, D., Bonan, G., Bondeau, A., Cescatti, A., Lasslop, G., Lindroth, A., Lomas, M., Luyssaert, S., Margolis, H., Oleson, K., Roupsard, O., Veenendall, E., Vivoy, N., Williams, C., Woodward, F., Papale, D. (2010). Terrestrial Gross Carbon Dioxide Uptake: Global Distribution and Covariation with Climate. *Science,329*(5993), 834-838. doi:10.1126/science.1184984

Cui, T., Wang, Y., Sun, R., Qiao, C., Fan, W., Jiang, G., Hao, L., Zhang, L. (2016). Estimating Vegetation Primary Production in the Heihe River Basin of China with Multi-Source and Multi-Scale Data. Plos One, 11(4). doi:10.1371/journal.pone.0153971

Field, C., & Mooney, H. A. (1983). Leaf age and seasonal effects on light, water, and nitrogen use efficiency in a California shrub. Oecologia, 56(2-3), 348-355. doi:10.1007/bf00379711

Gilmanov, T. G., Wylie, B. K., Tieszen, L. L., Meyers, T. P., Baron, V. S., Bernacchi, C. J., Billesbach, D., Burba, G., Fischer, M., Glenn, A., Hanan, N., Hatfield, J., Heuer, M., Hollinger, S., Howard, D., Matamala, R., Prueger, J., Tenuta, M., Young, D. G. (2013). CO2 uptake and ecophysiological parameters of the grain crops of midcontinent North America: Estimates from flux tower measurements. *Agriculture, Ecosystems & Environment*, 164, 162-175. doi:10.1016/j.agee.2012.09.017

Gitelson, A. A., Viña, A., Verma, S. B., Rundquist, D. C., Arkebauer, T. J., Keydan, G., Leavitt, B., Ciganda, V., Burba, G., Suyker, A. E. (2006). Relationship between gross primary production and chlorophyll content in crops: Implications for the synoptic monitoring of vegetation productivity. *Journal of Geophysical Research*, 111(D8). doi:10.1029/2005jd006017

Hazarika, M. K., Yasuoka, Y., Ito, A., & Dye, D. (2005). Estimation of net primary productivity by integrating remote sensing data with an ecosystem model. Remote Sensing of Environment, 94(3), 298-310. doi:10.1016/j.rse.2004.10.004

Heinsch, F. A., Reeves, M., Votava, P., Kang, S., Milesi, C., Zhao, M., Glassy, J., Jolly, W., Loehman, R., Bowker, C., Kimball, J., Nemani, R., Running, S. W. (2003, December 2). User's Guide GPP and NPP (MOD17A2/A3) Products NASA MODIS Land Algorithm [User's Guide for the MODIS GPP Product].

Heinsch, F., Zhao, M., Running, S., Kimball, J., Nemani, R., Davis, K., Bolstad, P., Cook, B., Desai, A., Ricciuto,D., Law, B., Kwon, H., Luo, ., Wofsy, S., Dunn, A., Munger, J., Baldocchi, D., Xu, L., Hollinger, D., Richardson, A., Stoy, P., Siqueira, M., Monson, R., Burns, S., Flanagan, L. (2006). Evaluation of remote sensing based terrestrial productivity from MODIS using regional tower eddy flux network observations. IEEE Transactions on Geoscience and Remote Sensing, 44(7), 1908-1925. doi:10.1109/tgrs.2005.853936

Kalfas, J. L., Xiao, X., Vanegas, D. X., Verma, S. B., & Suyker, A. E. (2011). Modeling gross primary production of irrigated and rain-fed maize using MODIS imagery and CO2 flux tower data. Agricultural and Forest Meteorology, 151(12), 1514-1528. doi:10.1016/j.agrformet.2011.06.007

Li, A., Bian, J., Lei, G., & Huang, C. (2012). Estimating the Maximal Light Use Efficiency for Different Vegetation through the CASA Model Combined with Time-Series Remote Sensing Data and Ground Measurements. Remote Sensing, 4(12), 3857-3876. doi:10.3390/rs4123857

Liu, J. (1997). A process-based boreal ecosystem productivity simulator using remote sensing inputs. Remote Sensing of Environment, 62(2), 158-175. doi:10.1016/s0034-4257(97)00089-8

Maselli, F., Papale, D., Puletti, N., Chirici, G., & Corona, P. (2009). Combining remote sensing and ancillary data to monitor the gross productivity of water-limited forest ecosystems. Remote Sensing of Environment, 113(3), 657-667. doi:10.1016/j.rse.2008.11.008

Matsushita, B., & Tamura, M. (2002). Integrating remotely sensed data with an ecosystem model to estimate net primary productivity in East Asia. Remote Sensing of Environment, 81(1), 58-66. doi:10.1016/s0034-4257(01)00331-5

Monteith, J. L. (1972). Solar Radiation and Productivity in Tropical Ecosystems. The Journal of Applied Ecology, 9(3), 747. doi:10.2307/2401901

Mourtzinis, S., Edreira, J. I., Conley, S. P., & Grassini, P. (2017). From grid to field: Assessing quality of gridded weather data for agricultural applications. European Journal of Agronomy, 82, 163-172. doi:10.1016/j.eja.2016.10.013

Nasahara, K. N. (2009). Simple Algorithm for Estimation of Photosynthetically Active Radiation (PAR) Using Satellite Data. Sola, 5, 37-40. doi:10.2151/sola.2009-010

Nguy-Robertson, A., Suyker, A., & Xiao, X. (2015). Modeling gross primary production of maize and soybean croplands using light quality, temperature, water stress, and phenology. Agricultural and Forest Meteorology, 213, 160-172. doi:10.1016/j.agrformet.2015.04.008

Nguy-Robertson, A. L., & Gitelson, A. A. (2015). Algorithms for estimating green leaf area index in C3 and C4 crops for MODIS, Landsat TM/ETM , MERIS, Sentinel MSI/OLCI, and Venμs sensors. Remote Sensing Letters, 6(5), 360-369. doi:10.1080/2150704x.2015.1034888

Raich, J. W., Rastetter, E. B., Melillo, J. M., Kicklighter, D. W., Steudler, P. A., Peterson, B. J., Grace III, A.L.B.M. Vorosmarty, C. J. (1991). Potential Net Primary Productivity in South America: Application of a Global Model. Ecological Applications, 1(4), 399-429. doi:10.2307/1941899

Reich, P. B., Walters, M. B., & Ellsworth, D. S. (1991). Leaf age and season influence the relationships between leaf nitrogen, leaf mass per area and photosynthesis in maple and oak trees. Plant, Cell and Environment, 14(3), 251-259. doi:10.1111/j.1365-3040.1991.tb01499.x

Sakamoto, T., Gitelson, A. A., Wardlow, B. D., Verma, S. B., & Suyker, A. E. (2011). Estimating daily gross primary production of maize based only on MODIS WDRVI and shortwave radiation data. Remote Sensing of Environment, 115(12), 3091-3101. doi:10.1016/j.rse.2011.06.015

Suyker, A. E., & Verma, S. B. (2012). Gross primary production and ecosystem respiration of irrigated and rainfed maize–soybean cropping systems over 8 years. Agricultural and Forest Meteorology, 165, 12-24. doi:10.1016/j.agrformet.2012.05.021

Wang, X., Ma, M., Huang, G., Veroustraete, F., Zhang, Z., Song, Y., & Tan, J. (2012). Vegetation primary production estimation at maize and alpine meadow over the Heihe River Basin, China. International Journal of Applied Earth Observation and Geoinformation, 17, 94-101. doi:10.1016/j.jag.2011.09.009

Weiss, A., & Norman, J. (1985). Partitioning solar radiation into direct and diffuse, visible and near-infrared components. Agricultural and Forest Meteorology, 34(2-3), 205-213. doi:10.1016/0168-1923(85)90020-6

Willmott, C. J. (1981). On the validation of models. Physical Geography, 2,2, 184-194. doi: 10.1080/02723646.1981.10642213

Wu, W., Wang, S., Xiao, X., Yu, G., Fu, Y., & Hao, Y. (2008). Modeling gross primary production of a temperate grassland ecosystem in Inner Mongolia, China, using MODIS imagery and climate data. Science in China Series D: Earth Sciences, 51(10), 1501-1512. doi:10.1007/s11430-008-0113-5

Xiao, X., Hollinger, D., Aber, J., Goltz, M., Davidson, E. A., Zhang, Q., & Moore, B. (2004). Satellite-based modeling of gross primary production in an evergreen needleleaf forest. Remote Sensing of Environment, 89(4), 519-534. doi:10.1016/j.rse.2003.11.008

Yu, Shaocai., Eder, Brian., Dennis, R., Chu, S., Schwartz, (n.d.) S.Statistics - Definitions and Issues Deriving “Unbiased Symmetric” Metrics. Retrieved March 28, 2017, from http://www.bing.com/cr?IG=43BE5CD8B55C4742920435E405126279&CID=339F2E1FCECC64BB3ED0244CCFFD657F&rd=1&h=pwmV_BU1vib9_ZNXqioln4D2FLG17AT0DK5PVcwCuqA&v=1&r=http%3a%2f%2fwww.ecd.bnl.gov%2fsteve%2fpres%2fmetrics.pdf&p=DevEx,5062.1

APPENDIX

Permission has been granted by Elsevier, the publisher of Agricultural and Forest Meteorology, to include the Nguy-Robertson et al., 2015 paper in the appendix of this thesis.

Order Completed

Thank you for your order.

This Agreement between Gunnar Malek-Madani ("You") and Elsevier ("Elsevier") consists of your license details and the terms and conditions provided by Elsevier and Copyright Clearance Center.

Your confirmation email will contain your order number for future reference.

Printable details.

License Number	4040860245312
License date	Feb 02, 2017
Licensed Content Publisher	Elsevier
Licensed Content Publication	Agricultural and Forest Meteorology
Licensed Content Title	Modeling gross primary production of maize and soybean croplands using light quality, temperature, water stress, and phenology
Licensed Content Author	Anthony Nguy-Robertson,Andrew Suyker,Xiangming Xiao
Licensed Content Date	November 2015
Licensed Content Volume	213
Licensed Content Issue	n/a
Licensed Content Pages	13
Type of Use	reuse in a thesis/dissertation
Portion	full article
Format	print
Are you the author of this Elsevier article?	No
Will you be translating?	No
Order reference number	
Title of your thesis/dissertation	Modeling Gross Primary Production of Maize and Soybean Croplands at a Regional Scale Using Remotely Sensed Data
Expected completion date	May 2017
Estimated size (number of pages)	30
Elsevier VAT number	GB 494 6272 12
Requestor Location	Gunnar Malek-Madani 2635 S 16th St LINCOLN, NE 68502 United States Attn: Gunnar Malek-Madani
Total	0.00 USD

ORDER MORE CLOSE WINDOW

Agricultural and Forest Meteorology 213 (2015) 160–172

Contents lists available at ScienceDirect

Agricultural and Forest Meteorology

journal homepage: www.elsevier.com/locate/agrformet

Modeling gross primary production of maize and soybean croplands using light quality, temperature, water stress, and phenology

Anthony Nguy-Robertson[a], Andrew Suyker[a,*], Xiangming Xiao[b,c]

[a] School of Natural Resources, University of Nebraska-Lincoln, Lincoln, NE, USA
[b] Center for Spatial Analysis, College of Atmospheric and Geographic Sciences, University of Oklahoma, Norman, OK, USA
[c] Department of Microbiology and Plant Biology, College of Arts and Sciences, University of Oklahoma, Norman, OK, USA

ARTICLE INFO

Article history:
Received 15 August 2014
Received in revised form 20 January 2015
Accepted 13 April 2015
Available online 14 July 2015

Keywords:
Gross primary production
Light use efficiency
Maize
Soybean
Modeling

ABSTRACT

Vegetation productivity metrics, such as gross primary production (GPP) may be determined from the efficiency with which light is converted into photosynthates, or light use efficiency (ϵ). Therefore, accurate measurements and modeling of ϵ is important for estimating GPP in each ecosystem. Previous studies have quantified the impacts of biophysical parameters on light use efficiency based GPP models. Here we enhance previous models utilizing four scalars for light quality (i.e., cloudiness), temperature, water stress, and phenology for data collected from both maize and soybean crops at three Nebraska AmeriFlux sites between 2001 and 2012 (maize: 26 field-years; soybean: 10 field-years). The cloudiness scalar was based on the ratio of incident photosynthetically active radiation (PAR_{in}) to potential (i.e., clear sky) PAR_{pot}. The water stress and phenology scalars were based on vapor pressure deficit and green leaf area index, respectively. Our analysis determined that each parameter significantly improved the estimation of GPP (AIC range: 2503–2740; likelihood ratio test: p-value < 0.0003, df = 5–8). Daily GPP data from 2001 to 2008 calibrated the coefficients for the model with reasonable amount of error and bias (RMSE = 2.2 g C m^{-2} d^{-1}; MNB = 4.7%). Daily GPP data from 2009 to 2012 tested the model with similar accuracy (RMSE = 2.6 g C m^{-2} d^{-1}; MNB = 1.7%). Modeled GPP was generally within 10% of measured growing season totals in each year from 2009 to 2012. Cumulatively, over the same four years, the sum of error and the sum of absolute error between the measured and modeled GPP, which provide measures of long-term bias, was ±5% and 2–9%, respectively, among the three sites.

1. Introduction

The efficiency of light converted into photosynthates, or light use efficiency (ϵ), is a useful measure of crop productivity (Monteith, 1972). Light use efficiency can be measured at the leaf (Garbulsky et al., 2013), plant (Onoda et al., 2014), or ecosystem/landscape level (Binkley et al., 2013). It is at the landscape level where light use efficiency is used as an important component of many ecosystem production models (e.g., Gilmanov et al., 2013; John et al., 2013) determining net and gross primary production (NPP and GPP, respectively). Therefore, accurate measurements and modeling of ϵ is important for estimating vegetation productivity in a variety of ecosystems. Many factors impact ϵ such as water content (e.g., Inoue and Peñuelas, 2006), nitrogen content (e.g., Peltoniemi et al., 2012), temperature (e.g., Hall et al., 2012), and CO_2 concentration (e.g., Haxeltine and Prentice, 1996). Because of the impacts of these factors, a maximum light use efficiency (ϵ_0) is typically used in ecosystem productivity models (e.g., Li et al., 2012) and downregulated as environmental conditions change. However, there are known assumptions and errors associated with using ϵ_0 (Xiao, 2006) and improvements in estimating light use efficiency is necessary to improve these ecosystem production models.

Incorporating light quality, a major factor impacting ϵ (Gu et al., 2003), has been shown to improve ecosystem productivity models (Knohl and Baldocchi, 2008; Suyker and Verma, 2012). This is due to the sensitivity of ϵ to the light climate in the canopy (He et al., 2013; Zhang et al., 2011). The light quality impact suggests ϵ should not be defined as a down-regulated maximum value, but as a clear sky value that decreases due to environmental stress and increases due to cloud cover. The light use efficiency has been shown to increase under diffuse light conditions (Gu et al., 2002) in relation to the ratio of diffuse (PAR_d) to incident photosynthetically active radiation (PAR_{in}) (Schwalm et al., 2006). As diffuse light

* Corresponding author at: 3310 Holdrege, Lincoln, NE 68583-0973, USA. Tel.: +1 402 472 2168; fax: +1 402 472 2946.
E-mail address: asuyker1@unl.edu (A. Suyker).

http://dx.doi.org/10.1016/j.agrformet.2015.04.008
0168-1923/

is not frequently measured, it would be advantageous to have an alternative to PAR_d/PAR_{in}. Turner et al. (2003) defined a cloudiness coefficient (CC) based on PAR_{in} and the clear-sky potential of photosynthetically active radiation (PAR_{pot}). The CC was used as a proxy for the quality of light affecting ϵ but not incorporated into their light use efficiency model.

The Vegetation Photosynthesis Model (VPM) is a light use efficiency model that utilizes remote sensing imagery to estimate GPP based on the impacts of temperature, water stress, and phenology (Xiao et al., 2004). These particular factors impact ϵ because (1) plants are affected but can recover quickly (i.e., short-term) from unfavorable temperatures (Crafts-Brandner and Law, 2000), (2) plants take longer to recover (i.e., long-term) from prolonged water stress (Miyashita et al., 2005; Souza et al., 2004), and (3) leaf age impacts photosynthesis rates (Reich et al., 1991). Richardson et al. (2012) indicated that accurate estimates of phenology were necessary for modeling productivity because errors can lead to large biases in cumulative estimates of GPP. In using satellite imagery, the VPM in most situations cannot be applied daily due to limited frequency of clear sky imagery and thus, would not include the impact of light quality on GPP estimates.

However, models incorporating satellite data (e.g., VPM) are critical in developing regional/global estimates of GPP (Yuan et al., 2010). In this study, we adapt a remote sensing-based light use efficiency model to in-situ meteorological (e.g., temperature, VPD) and biophysical data (e.g., green LAI) to estimate the impacts of temperature, water stress, and phenology on ϵ in order to estimate daily GPP. We note that with the development of gridded meteorological data sets (e.g., Maurer et al., 2002) and remotely sensed biophysical parameters (e.g., Nguy-Robertson et al., 2014), this approach could potentially be applicable on a daily basis at regional/global scales. In this study, our objectives are to (1) enhance the light use efficiency model estimation of GPP on a daily and seasonal basis utilizing four scalars for light quality, temperature, water stress, and phenology for in-situ data collected from both maize and soybean at three Nebraskan sites between 2001 and 2008 and (2) evaluate these models from crop data collected at these sites between 2009 and 2012 on a daily, seasonal, and multi-year basis.

2. Materials and methods

2.1. Study site summary

The study area included three fields located at the University of Nebraska-Lincoln (UNL) Agricultural Research and Development Center (ARDC) near Mead, Nebraska, U.S.A. The three sites belong to the AmeriFlux Network, which is sponsored by the U.S. Department of Energy, monitoring carbon fluxes across the North and South American continents. US-Ne1 (41.165°N, 96.4766°W, 361 m; 49 ha) and US-Ne2 (41.1649°N, 96.4701°W, 362 m; 52 ha) were equipped with a center pivot irrigation system while US-Ne3 (41.1797°N, 96.4396°W, 363 m; 65 ha) was rainfed. In 2001, the sites were prepared by disking the top 0.1 m of the soil to achieve a uniformly tilled surface that incorporated fertilizers as well as accumulated crop residues. US-Ne1 was planted as continuous maize and US-Ne2 and US-Ne3 were under a maize/soybean rotation (Table 1). After the initial tillage operation in 2001, the three sites were no-till until 2005 when US-Ne1 was tilled due to declining yields associated with the effects of high residue cover. Thus for US-Ne1, a conservation plow method, that does not completely invert the topsoil, was initiated in the fall of each year starting in 2005. In 2010, a biomass removal study was initiated where the management of US-Ne2 was changed to match US-Ne1 (continuous maize with tillage operations in the fall) except for one factor. Stover was baled and removed from US-Ne2 prior to tillage in order to study the impact of residue removal on carbon and water fluxes. All fields have been fertilized and treated with herbicide and pesticides following best management practices for Eastern Nebraska. For maize, in the irrigated fields, approximately 180 kg N ha^{-1} was applied each year. This was conducted in three applications using the center pivot. Approximately two-thirds (120 kg N ha^{-1}) was applied pre-planting and the remaining (60 kg N ha^{-1}) was applied in two fertigations. Only a single pre-plant N fertilizer application of 120 kg N ha^{-1} was made on the rainfed site during maize years. Table 1 summarizes the three study sites from 2001 to 2012 (e.g., yield, planting, emergence, and harvest dates).

2.2. Flux measurements

The eddy covariance flux measurements of CO_2 (F_c), latent heat (LE), sensible heat (H), and momentum fluxes were collected using a Gill Sonic anemometer (Model R3; Gill Instruments Ltd., Lymington, UK), a closed- and open-path CO_2/H_2O water vapor sensor (LI-6262 and LI-7500, respectively; LI-Cor Lincoln, NE). Storage of CO_2 below the eddy covariance sensors was determined from profile measurements of CO_2 concentration (LI-6262) and combined with F_c to determine net ecosystem productivity (NEP). Processing methods for correcting flux data due to coordinate rotation (e.g., Baldocchi et al., 1988), inadequate sensor frequency response (e.g., Massman, 1991), and variation in air density (Webb et al., 1980) were applied to all data sets. Key supporting meteorological variables measured included soil heat flux, humidity, incident solar radiation, in situ air and soil temperature, windspeed, and incident photosynthetically active radiation (PAR_{in}). Missing data due to sensor malfunction, unfavorable weather, power outages, etc., were gap-filled using a method that combined measurements, interpolation, and empirical data (Baldocchi et al., 1997; Kim et al., 1992; Suyker et al., 2003; Wofsy et al., 1993). Problems associated with insufficient turbulent mixing during nighttime hours was also corrected (Barford et al., 2001; Suyker and Verma, 2012). When mean windspeed (U) was below the threshold value ($U = 2.5\ m\ s^{-1}$ corresponding to a friction velocity of approximately 0.25 m s^{-1}), data were filled in using night CO_2 exchange-temperature relationships from windier conditions. The daytime estimates of ecosystem respiration (Re) were determined from the temperature-adjusted nighttime CO_2 exchange (Xu and Baldocchi, 2004). The GPP was obtained from the difference between NEP and Re (sign convention: GPP and NEP are positive during C uptake by the vegetation and Re is negative).

Energy budget closure is a known issue with regards to eddy covariance measurements and is due, in part, to errors associated with the angle of attack (Frank et al., 2013; Nakai et al., 2006) and phase shifts when estimating energy storage terms (Leuning et al., 2012). For this study, the energy budget closure was determined by comparing the sum of latent and sensible heat fluxes ($LE + H$) measured by eddy covariance methods with the sum of net radiation and energy storage ($R_n + G$). The growing season energy budget closures for all three sites from 2001 to 2012 (0.78–0.97) were reasonable considering the errors inherent in the measurements of these terms.

2.3. Other supporting measurements

Destructive leaf area measurements were collected from six small (20 × 20 m) plots (i.e., intensive measurement zones or IMZs). The IMZs represent all major soil types of each site, including Tomek, Yutan, Filbert, and Filmore soil series (Suyker et al., 2004). The green LAI, or photosynthetically active leaf area index, was calculated from a 1 m sampling length from one or two rows (6 ± 2 plants) within each IMZ. Samples were collected from each field every 10–14 days starting at the initial growth stages (Abendroth et al., 2011), and ending at crop maturity. To minimize edge

Table 1
Site information: year, site, crop, cultivars planted, planting density, day of year for planting/emergence/harvest, and yield at 15.5% and 13% moisture content for maize (M) and soybean (S), respectively. Yield indicated with "*" were reduced due to a hail event.

Site	Year	Crop/cultivar	Planting density (plants ha^{-1})	Day of year Planting	Emergence	Harvest	Yield (Mg ha^{-1})
US-Ne1	2001	M/Pioneer 33P67	81,500	130	136	291	13.51
	2002	M/Pioneer 33P67	71,300	129	138	308	12.97
	2003	M/Pioneer 33B51	77,000	135	147	300	12.12
	2004	M/Pioneer 33B51	79,800	124	134	289	12.24
	2005	M/DeKalb 63-75	69,200	124	137	286	12.02
	2006	M/Pioneer 33B53	80,600	125	136	278	10.46
	2007	M/Pioneer 31N30	75,300	121	130	309	12.8
	2008	M/Pioneer 31N30	76,500	120	130	323	11.99
	2009	M/Pioneer 32N73	78,500	110	125	313	13.35
	2010	M/DeKalb 65-63 VT3	78,700	109	124	264	2.03*
	2011	M/Pioneer 32T88	80,200	138	146	299	11.97
	2012	M/DeKalb 62-97 VT3	77,200	115	123	284	13.02
US-Ne2	2001	M/Pioneer 33P67	82,400	131	138	295	13.41
	2002	S/Asgrow 2703	3,33,100	140	148	280	3.99
	2003	M/Pioneer 33B51	78,000	134	145	296	14
	2004	S/Pioneer 93B09	2,96,100	154	160	292	3.71
	2005	M/Pioneer 33B51	76,300	122	134	290	13.24
	2006	S/Pioneer 93M11	3,07,500	132	143	278	4.36
	2007	M/Pioneer 31N28	77,600	122	131	310	13.21
	2008	S/Pioneer 93M11	3,18,000	136	146	283	4.22
	2009	M/Pioneer 32N72	76,500	111	126	314	14.18
	2010	M/DeKalb 65-63 VT3	70,000	110	133	259	4.68*
	2011	M/Pioneer 32T88	81,100	138	146	299	12.54
	2012	M/DeKalb 62-97 VT3	78,700	116	124	283	13.1
US-Ne3	2001	M/Pioneer 33B51	52,300	134	141	302	8.72
	2002	S/Asgrow 2703	3,04,500	140	148	282	3.32
	2003	M/Pioneer 33B51	57,600	133	142	286	7.72
	2004	S/Pioneer 93B09	2,64,700	154	160	285	3.41
	2005	M/Pioneer 33G66	53,700	116	131	290	9.1
	2006	S/Pioneer 93M11	2,84,600	131	142	281	4.31
	2007	M/Pioneer 33H26	55,800	122	133	304	10.23
	2008	S/Pioneer 93M11	3,13,000	135	146	282	3.97
	2009	M/Pioneer 33T57	60,500	112	127	315	12
	2010	S/Pioneer 93M11	2,51,200	139	147	279	4.14
	2011	M/DeKalb 61-72 RR	50,200	122	133	291	9.73
	2012	S/Pioneer 93M43	2,94,800	136	142	275	2.17

effects, collection rows were alternated between sampling dates. The plants collected were transported on ice to the laboratory where they were visually divided into green leaves, dead leaves, stems, and reproductive organs. The leaf area was measured using an area meter (Model LI-3100, LI-Cor Lincoln, NE). The values calculated from all six IMZs were averaged for each sampling date to provide a field-level green LAI. The daily green LAI measurements for maize and soybean were determined from using a spline interpolation function calculated between destructive sampling dates.

In each field, incident and reflected PAR sensors (Model LI-190; Li-Cor Inc., Lincoln, NE, USA) above the canopy and six light bars (LI-191; Li-Cor Inc., Lincoln, NE, USA) above the soil surface provided data to quantify PAR absorbed by the canopy (APAR). These values were used in conjunction with LAI measurements to determine an extinction coefficient (k) for each crop. To minimize noise and errors, the average value of k for each crop was determined using only points when green LAI was greater than 1.5 m^2 m^{-2} and dead LAI was less than 0.5 m^2 m^{-2}.

2.4. GPP modeling approach

A basic light use efficiency relationship is used to model GPP for each day of the growing season:

$$\mathrm{GPP} = \epsilon \times \mathrm{APAR} \quad (1)$$

where ϵ is the daily light use efficiency and APAR is the daily sum of light absorbed by the photosynthetically active (i.e., green) fraction of the canopy. The APAR is defined using the Beer–Lambert Law as:

$$\mathrm{APAR} = \mathrm{PAR_{in}} \times \left(1 - e^{-k \times \mathrm{greenLAI}}\right) \quad (2)$$

where k is the light extinction coefficient and green LAI is leaf area index participating in photosynthesis. While the total leaf area index will account for all light absorbed by the canopy, during leaf senescence, not all of this energy will be converted into photosynthates (Field and Mooney, 1983).

The daily light use efficiency has been modeled several different ways: using differences in sunlight vs. shaded leaves (He et al., 2013), temperature and light (McCallum et al., 2013), remote sensing models (Pei et al., 2013), etc. The Vegetation Photosynthesis Model (VPM; Xiao et al., 2004), which was originally developed for satellite imagery, scales ϵ using temperature (T_{scalar}), water stress (W_{scalar}), and phenology (P_{scalar}):

$$\epsilon = \epsilon_0 \times T_{\mathrm{scalar}} \times W_{\mathrm{scalar}} \times P_{\mathrm{scalar}} \quad (3)$$

where ϵ_o is maximum light use efficiency, Suyker and Verma (2012) scaled light use efficiency based on a light quality or amount of diffuse light (C_{scalar}):

$$\epsilon = \epsilon_0 \times C_{\mathrm{scalar}} \quad (4)$$

where ϵ_o is now defined as "clear sky" maximum light use efficiency. In this study, ϵ was scaled using all four scalars, light quality, temperature, water stress, and phenology:

$$\epsilon = \epsilon_0 \times C_{\mathrm{scalar}} \times T_{\mathrm{scalar}} \times W_{\mathrm{scalar}} \times P_{\mathrm{scalar}} \quad (5a)$$

Thus, daily GPP can be estimated using a cloud-adjusted light use efficiency model (LUE_c):

$$GPP = \epsilon_0 \times C_{scalar} \times T_{scalar} \times W_{scalar} \times P_{scalar} \times APAR \quad (5b)$$

The C_{scalar} takes into account improved efficiency of canopy photosynthesis in diffuse compared to direct light. Therefore, C_{scalar} scales above 1 using the following equation (Suyker and Verma, 2012):

$$C_{scalar} = 1 + \beta \times \left(\frac{PAR_d}{PAR_{in}} - 0.17\right) \quad (6)$$

where β is the sensitivity of ϵ to diffuse light and $PAR_d/PAR_{in} = 0.17$ on a clear day. However, at many research sites, PAR_d data are not collected. To incorporate the effect of diffuse light in this ϵ model, PAR_d/PAR_{in} was related to the cloudiness coefficient (CC):

$$CC = 1 - \frac{PAR_{in}}{PAR_{pot}} \quad (7a)$$

where PAR_{pot} is the estimated total amount of daily incident PAR assuming cloud-free conditions based on factors, such as latitude, elevation, atmospheric pressure, etc. (Weiss and Norman, 1985). We note corrected equations (A. Weiss, personal communication) for hourly PAR_{pot} as the sum of direct and diffuse PAR (R_{DV} and R_{dV}, respectively):

$$PAR_{pot} = R_{DV} + R_{dv} \quad (7b)$$

$$R_{DV} = 2428 \times \cos\theta \times \exp\left(\frac{-0.185 \times P}{101.325 \times \cos\theta}\right) \quad (7c)$$

$$R_{dv} = 0.4 \times (2428 \times \cos\theta - R_{DV}) \quad (7d)$$

where θ is solar zenith angle (midpoint of each hour), P is site atmospheric pressure (kPa), and PAR incident at the top of the atmosphere is 2428 $\mu mol\, m^{-2}\, s^{-1}$ (a value of 2760 was used in the original paper). Hourly values of PAR_{pot} were calculated and integrated over each day.

The T_{scalar} has been modeled based on the Terrestrial Ecosystem Model (Raich et al., 1991):

$$T_{scalar} = \frac{(T - T_{min}) \times (T - T_{max})}{[(T - T_{min}) \times (T - T_{max})] - (T - T_{opt})^2} \quad (8)$$

where T is daytime average air temperature (when PAR > 1 $\mu mol\, m^{-2}\, s^{-1}$) and the parameters for T_{min}, T_{max}, and T_{opt} were 10, 48, and 28 °C, respectively, based on Kalfas et al. (2011). While these temperature parameters could be more narrowly adapted to crop species (i.e., maize or soybean) or regions (i.e., eastern Nebraska), this broad temperature range should reduce the risk of the model becoming specific to a particular plant functional type (C_3 vs. C_4), growth stage, and/or region.

The W_{scalar} takes into account the complex impact of water stress on photosynthesis (i.e., changes in stomatal conductance, leaf water potential, etc.) caused by soil moisture and/or atmospheric water deficits. The W_{scalar} is determined using one of multiple techniques from remote sensing data (Wu et al., 2008) or meteorological variables (Maselli et al., 2009; Moreno et al., 2014). Vapor pressure deficit (VPD) is known to affect GPP over the course of a day (Pettigrew et al., 1990) and its impact increases in the presence of a soil moisture deficit (Hirasawa and Hsiao, 1999). The VPD is already used as a constraint for stomatal conductance in evapotranspiration models. For example, specific biomes are assign values of VPD, along with temperature, for when the stomata are expected to be fully open or closed and these values are applied to the model using look-up tables (Mu et al., 2011, 2007). A similar approach, using one set of VPD values for all crops, was adapted for ϵ models (Yuan et al., 2010). For our study, we modified an approach estimating the plant photosynthetic response to VPD based on varying convexity (Gilmanov et al., 2013). This approach has originally been used in examining changes where the scalar will remain stable (e.g., at 1) until VPD reaches a critical threshold (generally accepted near 1 kPA) that induces a reduction in photosynthesis (El-Sharkawy et al., 1984; Lasslop et al., 2010). However, for this study we seek to determine a scalar useful for daily averages of VPD. Since a daily average of VPD below 1 kPa could contain periods where VPD was greater than 1 kPa, no critcal threshold was utilized resulting in the following equation:

$$W_{scalar} = \exp\left\{-\left[\left(\frac{VPD}{\sigma_{W_{scalar}}}\right)^2\right]\right\} \quad (9)$$

where the $\sigma_{W_{scalar}}$ is the curvature parameter for water stress.

The P_{scalar}, determined using remote sensing techniques, accounts for the impact of phenology/leaf age at the canopy level (Kalfas et al., 2011; Wang et al., 2012). Immature leaves do not have the same capacity as mature leaves to photosynthesize (Reich et al., 1991) and mature leaves lose their photosynthetic capacity as they senesce (Dwyer and Stewart, 1986; Field and Mooney, 1983). Green LAI is a good indicator of canopy-level phenological changes in maize and soybean increasing during leaf expansion (vegetative growth stages) and decreasing as canopy chlorophyll is degraded (reproductive growth stages/senescence; Nguy-Robertson et al., 2012). For our study, the equation was adjusted such that the P_{scalar} was one at peak green LAI:

$$P_{scalar} = \exp\left\{-\left[\left(\frac{\text{green LAI}_{max} - \text{greenLAI}}{\sigma_{P_{scalar}}}\right)^2\right]\right\} \quad (10)$$

where the$\sigma_{P_{scalar}}$ is the curvature parameter for phenology and green LAI_{max} is the maximal green LAI for each rainfed and irrigated crop. Green LAI_{max} is a potential maximum leaf area for a particular crop management (e.g., irrigation, planting density). Other factors (e.g., extreme weather, plant pests/disease) can affect leaf area distribution and peak values in a particular year. These impacts on P_{scalar} are discussed in Section 3.1.

2.5. Statistical methods

The four LUE_c parameters ϵ_o, β, $\sigma_{W_{scalar}}$, and $\sigma_{P_{scalar}}$ were determined using a step-wise iterative, or "model tuning" approach (Dall'Olmo et al., 2003; Gitelson et al., 2006). While all four parameters could be determined by simultaneous iteration, it would be computationally intensive. Therefore, predetermined ranges of each parameter were established (maize: ϵ_o: 0.426–1.0 g C mol^{-1}, $\sigma_{W_{scalar}}$: 3–50 kPa, and $\sigma_{P_{scalar}}$: 6–50 $m^2\, m^{-2}$; soybean: ϵ_o: 0.298–1.0 g C mol^{-1}, $\sigma_{W_{scalar}}$: 3–50 kPa, and $\sigma_{P_{scalar}}$: 6–50 $m^2\, m^{-2}$) following a k-fold cross-validation procedure (Kohavi, 1995) where k was the number of field-years for each crop between 2001 and 2008: 16 for maize and 8 for soybean.

The step-wise process consisted of eight iterations. The first step was to estimate ϵ_o using the data when C_{scalar}, W_{scalar}, and P_{scalar} are assumed to be close to 1. Thus, ϵ_o was determined during sunny conditions (CC < 0.2) with low water stress (VPD < 1.0) and a relatively mature canopy (LAI > 2 $m^2\, m^{-2}$). After quantifying ϵ_o, the β was determined by using an expanded data set disregarding the limitation using the CC. Likewise, $\sigma_{W_{scalar}}$ was determined with all VPD values included. The fourth iteration isolated $\sigma_{P_{scalar}}$ using the entire data set. To ensure relative stability, the four iterations were repeated using the entire data set and the parameters identified in the first four steps. In order to make an accurate comparison between the approach in this study and the approach presented in Suyker and Verma (2012), the Suyker and Verma (2012) model utilized the original coefficients (i.e. k, ϵ_o, etc.) rather than the updated values (Table 2).

Table 2
Summary of the model constants (bold) and corresponding equation number (Eqs.) utilized in this study. Maximum green leaf area values unique to the rainfed site (US-Ne3) are indicated in square brackets.

	Suyker and Verma (2012)		This study				
Constants	**Symbol**	**Eqs.**	**Units**	**Maize**	**Soybean**	**Maize**	**Soybean**
light extinction coefficient	k	(2)	Unitless	0.484	0.576	**0.443**	**0.601**
maximal light use efficiency	ϵ_0	(3)-(5)	g C mol^{-1}	0.426 ± 0.022	0.298 ± 0.013	**0.526 ± 0.007**	**0.374 ± 0.005**
sensitivity of ϵ to diffuse light	β	(6), (13)	Unitless	0.487 ± 0.19	0.877 ± 0.184	**0.347 ± 0.051**	**0.411 ± 0.056**
minimum temperature for physiological activity	T_{min}	(8)	°C			**10**	**10**
maximum temperature for physiological activity	T_{max}	(8)	°C			**48**	**48**
optimal temperature for physiological activity	T_{opt}	(8)	°C			**28**	**28**
water stress curvature parameter	$\sigma_{W_{scalar}}$	(9)	kPa			**6 ± 0.25**	**4 ± 0**
maximal green leaf area index	green LAI$_{max}$	(10)	m^2 m^{-2}			**6.78[4.93]**	**6.15[4.63]**
phenology curvature parameter	$\sigma_{P_{scalar}}$	(10)	m^2 m^{-2}			**18 ± 4.59**	**18 ± 7.15**

The optimal parameters were selected based on a minimum sum of absolute error (MSAE) regression (André et al., 2003; Narula et al., 1999) using R (V. 3.0.1, 2013, The R Foundation for Statistical Computing). MSAE regression has been found to be advantageous when there are outliers in the data set and the median is a more efficient estimator of the parameter rather than the mean (Narula et al., 1999). Due to differences between fields and various climatic conditions, the annual sum of GPP at a given site can be drastically different from normal years. This difference then impacts the mean value of the annual sum of GPP (maize: median = 1669 g C m^{-2}, average = 1641 g C m^{-2}; soybean: median = 916 g C m^{-2}, average = 944 g C m^{-2}). The sum of absolute error (SAE) by field-year (SAE$_{field\text{-}year}$) reduces both error and bias because self-correcting errors in the annual (i.e., field-year) sums were penalized. Thus, this approach minimizes the absolute value of the annual difference between modeled and measured GPP for a given site:

$$SAE_{field-year} = \Sigma_{field-year}|\Sigma_{Daily}\text{EstimatedGPP} - \Sigma_{Daily}\text{ModeledGPP}| \quad (11)$$

The approach minimizing SAE$_{field\text{-}year}$ also accentuates annual over daily performance in the model. A SAE analyses for daily values would over-emphasize accuracy for high GPP values. Basic statistical analyses were performed using Excel (V. 2010, Microsoft) where the coefficients of determination (R^2) were calculated from the best-fit lines and the mean normalized bias (MNB), and root mean square (RMSE) were calculated from the 1:1 line.

When incorporating a new factor into the VPM (C_{scalar}) and modifying other scalars (T_{scalar}, W_{scalar}, and P_{scalar}), their statistical significance must be evaluated in explaining the variability in daily GPP. Since LUE$_c$ is non-linear, the model was transformed logarithmically to perform two separate model selection analyses, Akaike information criterion (AIC) and likelihood ratio test, in R (V. 3.0.1, 2013, The R Foundation for Statistical Computing). To determine if each scalar statistically improves the model we used the following process. From the base model (GPP = $\epsilon_0 \times$ APAR), the AIC was used to determine which singular scalar improved the model the most. The model with the lowest AIC values among the tested models will have the optimal number of parameters for explaining the data while minimizing complexity (Akaike, 1974; Held and Sabanés Bové, 2014). The likelihood ratio test identified if the model was significantly improved. The likelihood ratio test compares a simple model with a nested and more complex model to provide a measure of statistical significance to any improvement of the model by adding a parameter (Fischer, 1921; Held and Sabanés Bové, 2014). The optimal parameter at each level of complexity (i.e., number of scalars), determined from AIC, was used as the simpler model in the likelihood ratio test for the increasingly complex model up to the proposed cloud-adjusted light use efficiency model (LUE$_c$).

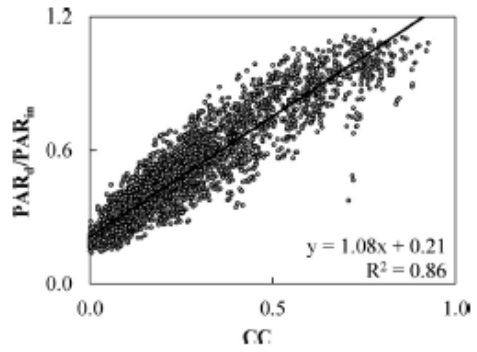

Fig. 1. The ratio of the incident photosynthetically active radiation (PAR$_{in}$) and diffuse PAR (PAR$_d$) in relation to cloudiness coefficient (CC) calculated from US-Ne1, US-Ne2, and US-Ne3 during growing seasons from 2001 to 2012 (n = 3879).

3. Results and discussion

3.1. Determination of model parameters

This study employed updated k values from Suyker and Verma (2012) to reflect the additional four years of APAR and LAI data collected at the site (8 vs. 12 years). The k was 0.444 for maize and 0.601 for soybean. These and other constants used in the model are in Table 2. The strong relationship between daily CC and daily PAR$_d$/PAR$_{in}$ (R^2 = 0.86; Fig. 1) allows for the following relationship to be used in lieu of diffuse light measurements:

$$\frac{PAR_d}{PAR_{in}} = 1.08 \times CC + 0.21 \quad (12)$$

Thus, C_{scalar} can be represented as a combination of Eqs. (6) and (12):

$$C_{scalar} = 1 + \beta \times (1.08 \times CC - 0.04) \quad (13)$$

The values of ϵ_0, β, $\sigma_{W_{scalar}}$, and $\sigma_{P_{scalar}}$ were determined iteratively (see Section 2.4 for details). For maize and soybean, ϵ_0 was 0.526 ± 0.007 and 0.374 ± 0.005 g C mol^{-1}, respectively (Table 2, Fig. 2). A range of ϵ_0 values have been published in the literature (Table 3) from both ground-based and satellite derived studies (e.g., Prince and Goward, 1995; Yan et al., 2009; Cheng et al., 2014). The large variation of ϵ_0 across multiple studies may be due, in part, to incorporating different scaling factors and variations in how these scalars are modeled (e.g., VPD vs. land surface water index, LSWI, to estimate water stress). The β was originally determined in Suyker and Verma (2012) from regression as 0.487 ± 0.190 and 0.877 ± 0.184 for irrigated maize and soybean, respectively (from 2005 to 2006 at US-Ne1 and US-Ne2). In this

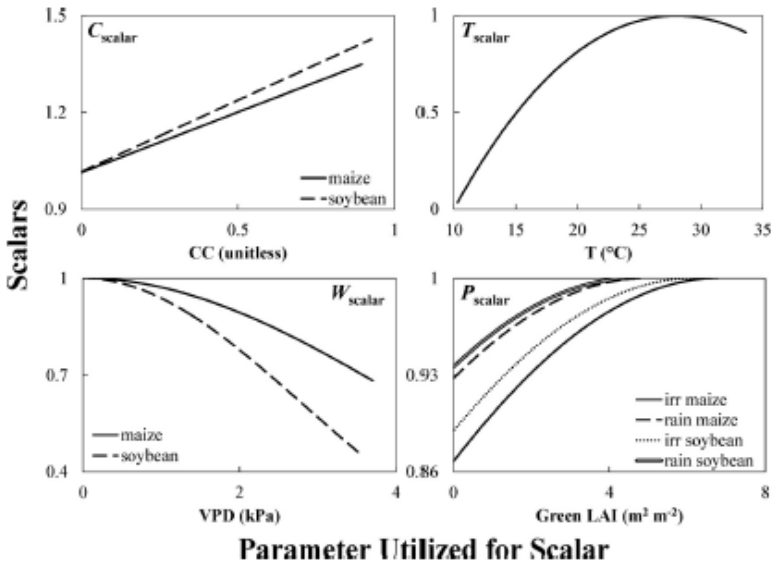

Fig. 2. The relationships between the parameters utilized for the scalars; cloudiness coefficient (CC), average daytime temperature (T), vapor pressure deficit (VPD), and green leaf area index (green LAI); and the scalars; C_{scalar}, T_{scalar}, W_{scalar}, P_{scalar}. Summary statistics for each parameter and scalar are in Table 4.

Table 3
Maximal light use efficiency (ϵ_o) values in units of g C mol^{-1} determined by various studies. For Prince and Goward (1995), the ϵ_o is adjusted by a temperature factor (α).

Reference	Year	Maize	Soybean	Developed specifically for maize or soybean?
Running et al.	2004	0.148	0.148	No
Cheng et al.	2014	0.915	0.567	Yes
Cheng et al.	2014	1.207	0.612	Yes
He et al.	2013	0.631		No
Kalfas et al.	2011	1.500		No
Lobell et al.	2002	0.4–0.8	0.4–0.8	No
Mahadevan et al.	2008	0.900	0.768	Yes
Norman and Arkebauer	1991	0.457–0.486	0.356–0.379	Yes
Prince and Goward	1995	0.600	12α	No
Suyker and Verma	2012	0.426	0.298	Yes
Wang et al.	2010	0.560		Yes
Wang et al.	2012	0.578		Yes
Yan et al.	2009	0.920		Yes
This study		0.526	0.374	Yes

study we determined β to be 0.347 ± 0.051 and 0.411 ± 0.056 for maize and soybean, respectively. This discrepancy was likely due to differences in model calibration. The original determination of β was from a single site in a single year for each crop. This study determined β using the entire calibration data set (24 field-years). The σw_{scalar} was determined to be 6 ± 0 and 4 ± 0 kPa for maize and soybean, respectively. The $\sigma_{P_{scalar}}$ was determined to be 18 ± 5 and 18 ± 7 m^2 m^{-2} for maize and soybean, respectively. The wide range in the variation using the k-fold cross-validation technique may be due to fitting the same $\sigma_{P_{scalar}}$ for both irrigated and rainfed crops despite the different maximal green LAI values. However, other factors not incorporated into the model can also impact green LAI (e.g., disease, damage by pests) and increase the uncertainty in the $\sigma_{P_{scalar}}$.

The resulting range of values for the scalars and other parameters are shown in Table 4. While the average for each scalar was close to one (0.9–1.1), on particular days the impact of some individual scalars was substantial. The temperature severely reduced ϵ on some days for both maize and soybean (T_{scalar} = 0.02–0.05) which occurred towards the end of the season when daily daytime temperature averages reached the minimum of 10 °C necessary for physiological activity. The lowest values for the W_{scalar} was in the rainfed soybean (0.46) when VPD was high (>3 kPa). However, this was relatively infrequent for all three sites (n = 36 days). The relatively small range of P_{scalar}, (~0.7–1.0) was expected as young leaves and canopies can photosynthesize, even if they are inefficient compared to fully mature leaves. This narrow range and the uncertainty in quantifying green LAI during later reproductive stages (Gitelson et al., 2014; Peng et al., 2011) may have contributed to the wider confidence intervals associated with the curvature parameter, $\sigma_{P_{scalar}}$. Despite multiple factors that reduce maximal green LAI for maize and soybean for their respective management, the P_{scalar} approached one each field-year (>0.985). The C_{scalar} increased to a maximum of 1.4 in both crops, supporting earlier studies demonstrating that cloudy conditions increase ϵ (e.g., Knohl and Baldocchi, 2008).

3.2. Model selection analysis, calibration, and validation

The LUE_c was developed using the 2001–2008 data. The likelihood ratio test demonstrated that each successive scalar, while adding complexity to the basic model, significantly improved the

Table 4
Summary of the parameters and corresponding equation number (Eq.) utilized in this study. The minimum (min), maximum (max), and average (avg) of each parameter was presented for each crop. Numbers in square brackets indicate values for the rainfed site (US-Ne3) while those to the left were for the two irrigated sites (US-Ne1 and US-Ne2).

				Maize			Soybean		
Parameters	Symbol	Eqs.	Units	Min	Max	Avg	Min	Max	Avg
Gross primary production	GPP	(1)	$g C m^{-2} d^{-1}$	0.0	33.5[29.5]	13.5[12.0]	0.0	18.7[19.6]	8.7[8.4]
Green leaf area index	green LAI	(2), (10)	$m^2 m^{-2}$	0.0	6.78[4.93]	3.26[2.35]	0.0	6.15[4.63]	2.36[1.91]
Absorbed PAR by green components	APAR	(2)	Mol photos $m^{-2} d^{-1}$	0.0	60.5[54.4]	28.4[24.7]	0.0	53.6[52.2]	24.9[24.3]
Incident PAR	PAR_{in}	(2)	Mol photos $m^{-2} d^{-1}$	1.0[1.4]	65.1[64.9]	30.9[31.0]	1.9[2.0]	63.4[62.8]	30.8[31.3]
Ratio of diffuse PAR and PAR_i	PAR_{di}/PAR_{in}	(6), (12)	Unitless	0.0	1.14[1.08]	0.48[0.49]	0.15	1.11[1.09]	0.49[0.48]
Cloudiness coefficient	CC	(7), (12), (13)	Unitless	0.0	0.90[0.89]	0.25	0.0	0.93[0.92]	0.25[0.24]
Potential PAR_{in}	PAR_{pot}	(7)	Mol photos $m^{-2} d^{-1}$	27.6	65.5	54.2	27.6	65.5	54.2
Temperature	T	(8)	°C	10.4[10.3]	33.6[33.2]	24.3[24.6]	12.9[10.9]	33.5	24.0[24.5]
Vapor pressure deficit	VPD	(9)	kPA	0.0[0.03]	3.52[3.70]	1.22[1.32]	0.0[0.06]	3.36[3.55]	1.13[1.33]
Cloudiness scalar	C_{scalar}	(6), (13)	Unitless	1.01[1.02]	1.35	1.11	1.02	1.43	1.13[1.12]
Temperature scalar	T_{scalar}	(8)	Unitless	0.04	1.0	0.92	0.31[0.10]	1.0	0.91[0.92]
Water stress scalar	W_{scalar}	(9)	Unitless	0.71[0.68]	1.0	0.95	0.49[0.45]	1.0	0.91[0.88]
Phenology scalar	P_{scalar}	(10)	Unitless	0.87[0.93]	1.0	0.95[0.97]	0.89[0.94]	1.0	0.95[0.97]

Table 5
Summary of model selection results for the Akaike Information Criterion (AIC) and likelihood ratio test. The difference between the AIC and minimum Akaike Information Criterion (AIC_{min}) was shown to make it easier to identify optimal models at each level of complexity. The optimal parameter at each level of complexity (in bold) was used as the simpler model in the likelihood ratio test for the increasingly complex model up to the proposed cloud-adjusted light use efficiency model (LUE_c). These results indicate that the addition of each remaining parameter was statistically significant (p-value < 0.001).

	Akaike information criterion		Likelihood ratio test	
Model	AIC	AIC-AICmin	p-value	df
$APAR \times \epsilon_o$	7065	4563		
$APAR \times \epsilon_o \times C_{scalar}$	2694	191	<0.0001	5
$APAR \times \epsilon_o \times T_{scalar}$	2735	233	<0.0001	5
$APAR \times \epsilon_o \times W_{scalar}$	2740	238	<0.0001	5
$APAR \times \epsilon_o \times P_{scalar}$	**2676**	**174**	**<0.0001**	**5**
$APAR \times \epsilon_o \times P_{scalar} \times C_{scalar}$	2637	134	<0.0001	6
$APAR \times \epsilon_o \times P_{scalar} \times T_{scalar}$	**2598**	**96**	**<0.0001**	**6**
$APAR \times \epsilon_o \times P_{scalar} \times W_{scalar}$	2652	150	<0.0001	6
$APAR \times \epsilon_o \times P_{scalar} \times T_{scalar} \times C_{scalar}$	**2528**	**25**	**<0.0001**	**7**
$APAR \times \epsilon_o \times P_{scalar} \times T_{scalar} \times W_{scalar}$	2532	30	<0.0001	7
LUE_c	**2503**	**0**	**0.0003**	**8**

estimation of daily GPP (p-value = 0.0002, df = 8; Table 5). The largest decrease in AIC occurred when adding any one of the scalars and the P_{scalar} contributed the most to the variability in GPP for these maize and soybean crops. The model estimated GPP with reasonable accuracy and low bias (RMSE: 2.2 g C $m^{-2} d^{-1}$; MNB: 4.7%; Fig. 3A). Minimizing bias has two benefits. Firstly, error due to bias will compound over time and thus reduce the accuracy in monitoring long-term trends in GPP. Secondly, lower bias indicates that over- and/or under-estimation of GPP was minimized for specific periods of the growing season (i.e., early, peak, etc.). The daily trends of the measured and modeled GPP between 2001 and 2008 roughly matched for US-Ne1 (Fig. 4), US-Ne2 (Fig. 5), and US-Ne3 (Fig. 6). This indicates that the model was reasonably estimating both low and high values of GPP.

The model was tested using the 2009–2012 data by evaluating daily and yearly RMSE and bias. While there was slightly

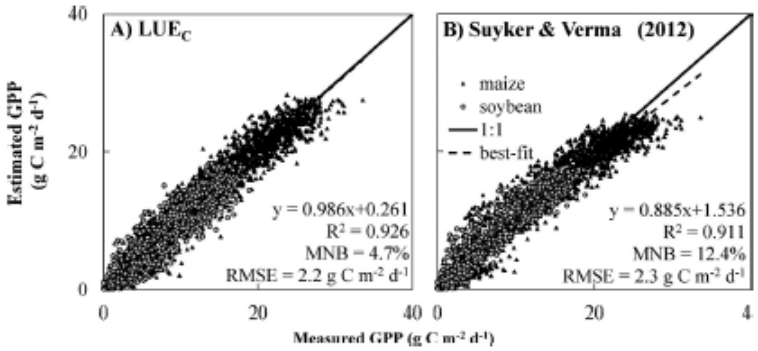

Fig. 3. The estimated and measured gross primary production (GPP) relationships from the 2001–2008 calibration data for the two light use efficiency models: (A) cloud-adjusted (LUE_c) and (B) Suyker and Verma (2012) model. The coefficient of determination (R^2) was determined from the best-fit line for maize and soybean data combined. The mean normalized bias (MNB) and root mean square error (RMSE) was determined from the 1:1 line.

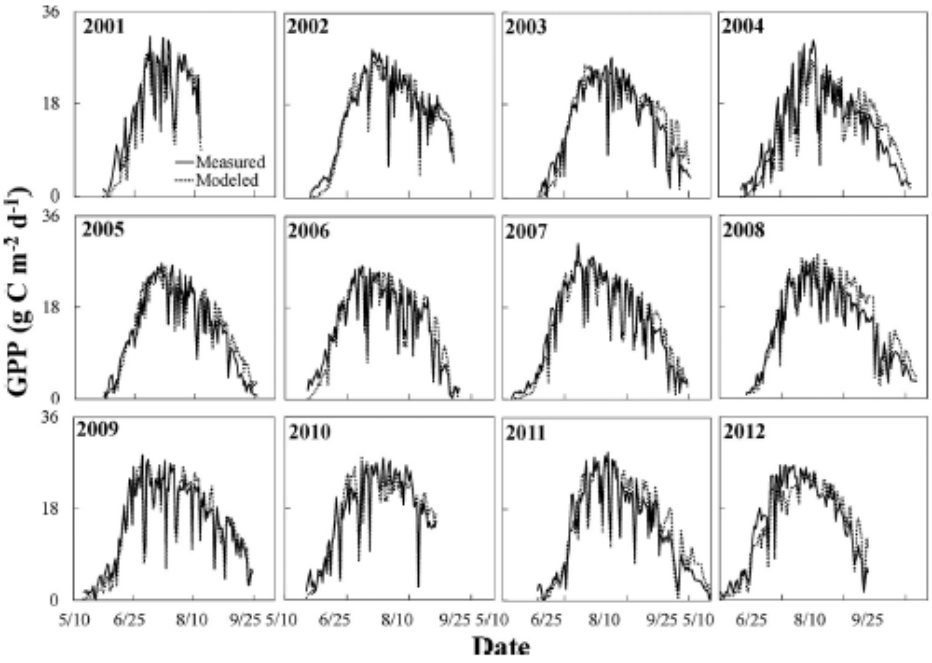

Fig. 4. Growing season distributions of the measured daily gross primary production (GPP) and the estimated GPP from the cloud-adjusted light use efficiency model (LUE_c) at the AmeriFlux site US-Ne1 located near Mead, NE, USA from 2001 to 2012. The site was managed as irrigated continuous maize during the entire study.

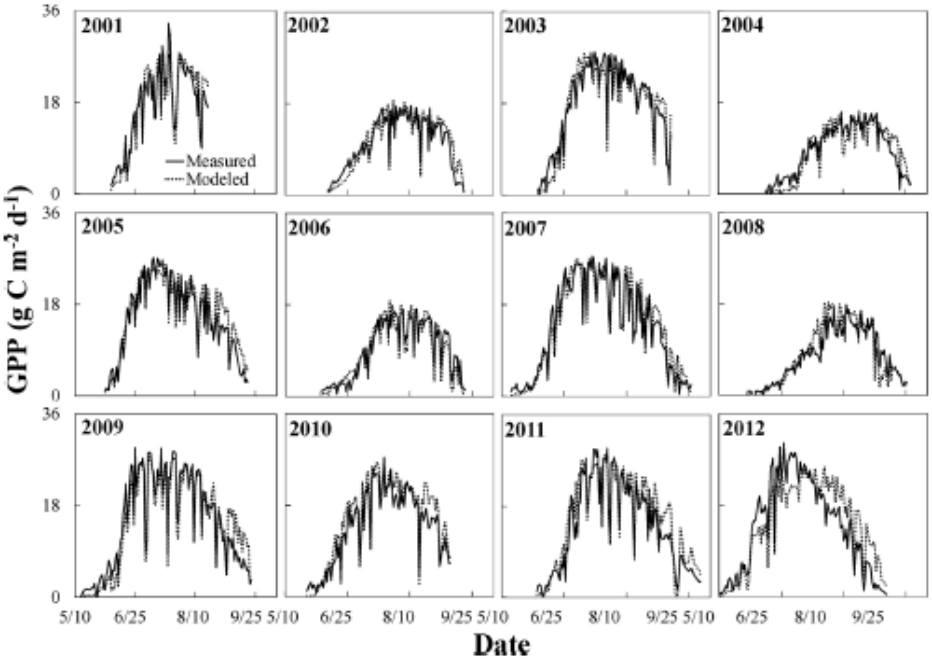

Fig. 5. Growing season distributions of the measured daily gross primary production (GPP) and the estimated GPP from the cloud-adjusted light use efficiency model (LUE_c) at the AmeriFlux site US-Ne2 located near Mead, NE, USA from 2001 to 2012. The site was irrigated and managed as a maize (odd years) and soybean (even years) rotation from 2001 to 2009. From 2010 to 2012 the site was managed as continuous maize.

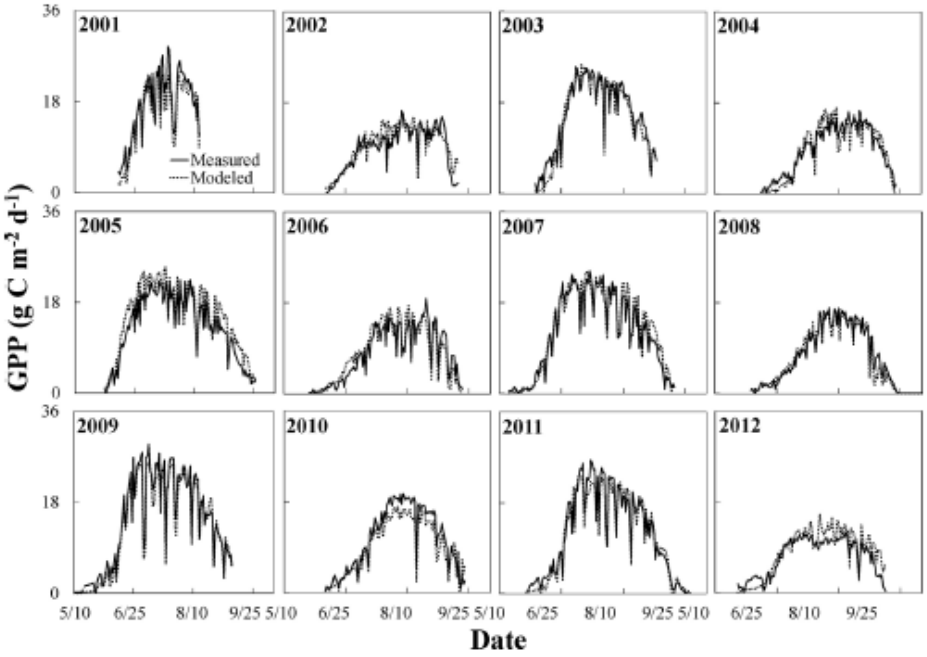

Fig. 6. Growing season distributions of the measured daily gross primary production (GPP) and the estimated GPP from the cloud-adjusted light use efficiency model (LUE_c) at the AmeriFlux site US-Ne3 located near Mead, NE, USA from 2001 to 2012. The site was rainfed and managed under a maize (odd years) and soybean (even) rotation.

increased scatter in the daily modeled vs. measured GPP relationships (RMSE = 2.6 g C m^{-2} d^{-1}), this error was still reasonable (Fig. 7A). The temporal behavior of the modeled and measured GPP for 2009–2012 was similar to those in 2001–2008 (Figs. 4–6). Yearly estimates of GPP (RMSE = 27.4 g C m^{-2} y^{-1}) were also reasonable (Fig. 7C). Desai et al. (2008) found the errors associated with the method of measuring GPP and gap-filling to be less than 10% across several methods in various biomes. For LUE_c all the data points in the validation data set fell within this 10% error threshold from measured GPP except for US-Ne3 in 2010 (13.5%) and 2012 (−13.5%).

The accuracy of the LUE_c over the period of validation (2009–2012) was strikingly good even with a change in management for US-Ne2 (from maize/soybean rotation to continuous maize) to accommodate a biomass study and several unforeseen events that influenced crop growth and the carbon flux. For example, at the end of the 2010 growing season there was a hail storm that damaged all three sites, but impacted US-Ne1 the most with an estimated loss of grain carbon of over 400 g C m^{-2} (stalks were lodged by large hail). This grain was incorporated in the field following fall conservation tillage to decompose the following growing seasons, yet this additional respiration did not impact GPP estimates for LUE_c (US-Ne1 2011; RMSE = 2.4 g C m^{-2} d^{-1}). Another unexpected event was the drought in 2012. While the LUE_c performed worse in 2012 compared to other years in several metrics (2012: RMSE = 3.4 g C m^{-2} d^{-1}; MNB = 13.5%), the model still had less error and bias than the Suyker and Verma (2012) model (2012: RMSE = 3.9 g C m^{-2} d^{-1}; MNB = 30.0%). This indicates that the LUE_c was fairly robust even during extreme events, likely due to using VPD as a metric for estimating the W_{scalar}.

In addition to evaluating the LUE_c and the significance of each parameter scaling ϵ, we also wanted to quantify the improvement in this model compared to Suyker and Verma (2012). The Suyker and Verma (2012) modeled values underestimated daily GPP compared to measured values for the developmental period (slope = 0.885 from 2001 to 2008; Fig. 3B) and the test period (slope = 0.839 from 2009 to 2012; Fig. 7B). Growing season totals show larger RMSE, too (Fig. 7D). Generally for all metrics utilized in this study (i.e., error, bias), the approach incorporating four scalars outperformed the single scalar based model. This suggests multiple factors are significantly impacting light use efficiency that ultimately affects daily and seasonal estimates of GPP.

3.3. Long-term error accumulation and bias associated with the models

While the daily accuracy of the model is important, small biases in modeled GPP can accumulate over multiple years. There are two types of cumulative error that reflect the quality of the model: (1) error that is self-correcting where over-estimations in some years can be offset by under-estimations in subsequent years which reduces bias (sum of error; SOE) and (2) error that accumulates the absolute difference between modeled and measured GPP each year (sum of absolute error; SAE). For the LUE_c from 2009 to 2012 for all three sites under differing management practices (e.g., rainfed vs. irrigated, continuous maize vs. maize/soybean rotation), the magnitude of SOE (US-Ne1: −33.7; US-Ne2: 272.7; US-Ne3: −231.4 g C m^{-2}) was within ±5% of measured cumulative GPP. The values of SAE ranged from 2 to 9% of GPP (US-Ne1: 157.0; US-Ne2: 398.5; US-Ne3 441.2 g C m^{-2}). The cumulative error and bias of LUE_c were within reason when compared to other light use efficiency models. For example, a direct comparison across the three sites, the SOE and SAE from the Suyker and Verma (2012) model ranged from −2 to 4% and 3 to 13%, respectively. The LUE_c demonstrates that it reduces self-correction compared to the earlier approach by Suyker and Verma (2012). Using the VPM between 2001 and 2005,

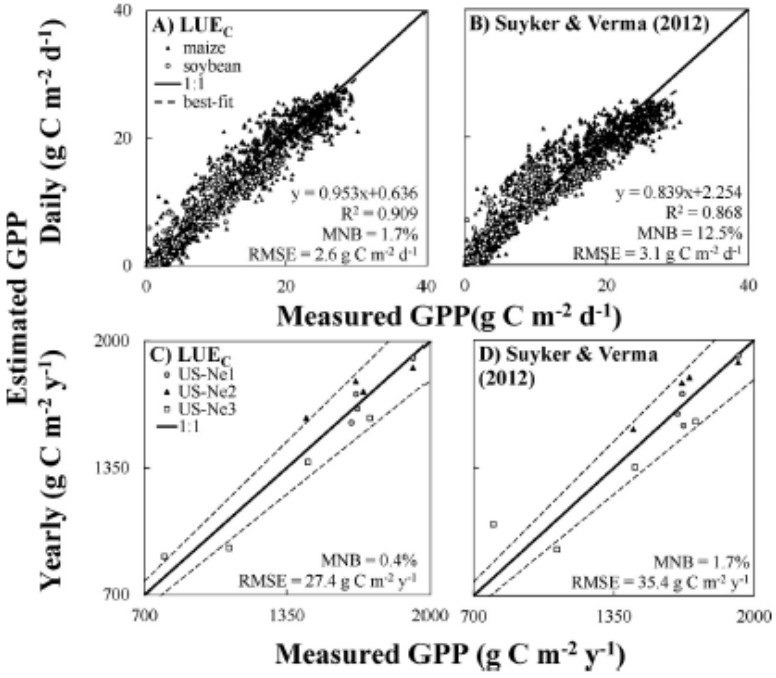

Fig. 7. The (A–B) daily and (C–D) yearly estimated vs. measured gross primary production (GPP) relationships from the 2009–2012 validation data set for the two light use efficiency models, (A,C) cloud-adjusted (LUE_c) and (B,D) Suyker and Verma (2012) model. The coefficient of determination (R^2) was determined from the best-fit line for both maize and soybean. The mean normalized bias (MNB) and root mean square error (RMSE) was determined from the 1:1 line. Ten percent error bars (dashed lines) are included in the yearly estimated GPP graphs.

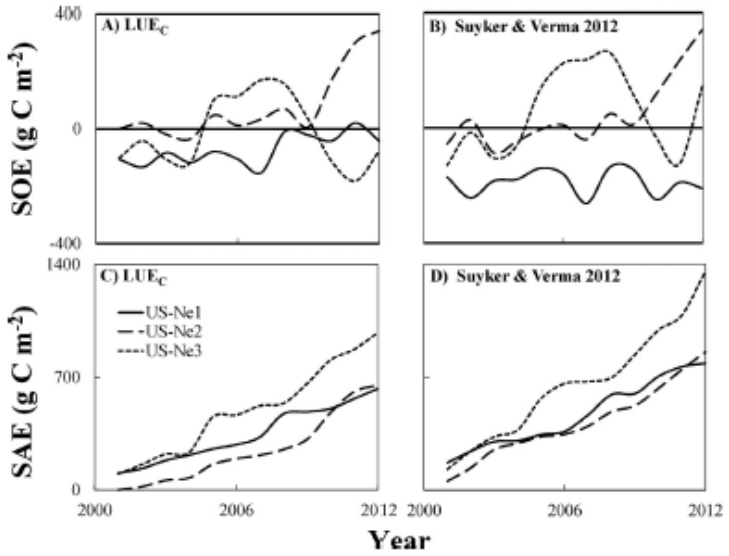

Fig. 8. Cumulative annual sum of error (SOE) between measured and estimated gross primary production (GPP) from 2001 to 2012 for (A) the cloud adjusted light use efficiency model (LUE_c) and (B) the Suyker and Verma (2012) model and cumulative annual sum of absolute error (SAE) for (C) LUE_c and (D) Suyker and Verma (2012) model.

Xiao et al., (2014) over-estimated GPP in each year for US-Ne2 for a total of 458 g C m^{-2} (SOE = SAE = 7%).

While the long-term analysis here is limited to four years, we repeated the analysis with data from 2001 to 2012 (Fig. 8A and C). Inclusion of the calibration data into this error analysis may not be ideal; however, it does provide some additional insights to the long-term trends. The SOE was −0.5 to 2% and SAE was 3 to 7% for all three sites where cumulative GPP measured 14,000 to 20,000 g C m^{-2}. The corresponding SOE and SAE for Suyker and Verma (2012) was −1 to 2% and 4 to 10%, respectively (Fig. 8B and D). From 2001 to 2005 at US-Ne2, the SOE and SAE were lower (0.7 and 2%, respectively) compared to Xiao et al., (2014). This error analysis suggests incorporating multiple scaling factors (regulated by meteorological and biophysical variables) into light use efficiency models can provide long-term GPP estimates with small bias.

4. Conclusion

The cloud-adjusted light use efficiency model (LUE_c) was able to model GPP utilizing field-based meteorological and biophysical measurements from three Nebraska AmeriFlux sites growing two different crops, maize and soybean, from 2001 to 2012. This light use efficiency (ϵ) model incorporated four scalars for estimating GPP; light climate, impacts of temperature, water stress, and phenology. The model coefficients for LUE_c were calibrated using a *k*-fold cross-validation procedure using data collected between 2001 and 2008. A computationally efficient iterative procedure ascertained initial parameter estimates from a limited range of environmental conditions and final parameters were determined from the entire data set. The likelihood ratio test demonstrated that all four scalars were statistically significant in improving the model estimation of daily GPP. On a day to day basis, temperature scalar can range from zero to one while the phenology scalar has the smallest range (0.7–1). However, based on the Akaike Information Criterion analysis, phenology explained more GPP variability compared to temperature and the other two scalars.

This model was validated on data collected between 2009 and 2012. The LUE_c had low error and bias estimates for daily and growing season GPP. On a cumulative basis, the sum of error between the measured and modeled GPP, which provides a measure of long-term cumulative bias (2001–2012), was less than 350 g C m^{-2} among the three sites. This is small considering 14,000 to over 20,000 g C m^{-2} of carbon had accumulated through GPP in maize and soybean crops. The performance of the LUE_c remained reasonable even during unusual events such as a change in management for US-Ne2 from 2010 to 2012, additional carbon input from a hailstorm in 2010, and an intense drought in 2012. Future research is necessary to determine if the parameters identified in this study are robust for regions outside of Eastern Nebraska. It would also be beneficial if this approach using four scalars for estimating ϵ could be adapted for regional and global estimates of GPP.

Acknowledgements

The US-Ne1, US-Ne2, and US-Ne3 AmeriFlux sites were supported by the DOE Office of Science (BER; Grant Nos. DE-FG03-00ER62996, DE-FG02-03ER63639, and DE-EE0003149), DOE-EPS-CoR (Grant No. DE-FG02-00ER45827), and NASA NACP (Grant No. NNX08AI75G). We are grateful to be supported by the resources, facilities, and equipment by the Carbon Sequestration Program, the School of Natural Resources, and the Nebraska Agricultural Research Division located within the University of Nebraska-Lincoln. We would like to thank Dr. Tim Arkebauer and Dave Scoby for the destructive leaf area measurements. We gratefully acknowledge the technical assistance of Sheldon Sharp, Ed Cunningham, Brent Riehl, Tom Lowman, Todd Schimelfenig, Dan Hatch, Jim Hines, and Mark Schroeder.

References

Abendroth, L.J., Elmore, R.W., Boyeer, M.J., Marlay, S.K., 2011. Corn Growth and Development. Iowa State University Extension, Ames, IA.
Akaike, H., 1974. A new look at the statistical model identification. IEEE Trans. Automat. Contr. 19, 716–723, http://dx.doi.org/10.1109/TAC1974.1100705
André, C.D.S., Narula, S.C., Elian, S.N., Tavares, R.A., 2003. An overview of the variables selection methods for the minimum sum of absolute errors regression. Stat. Med. 22, 2101–2111, http://dx.doi.org/10.1002/sim.1437
Baldocchi, D.D., Hincks, B.B., Meyers, T.P., 1988. Measuring biosphere-atmosphere exchanges of biologically related gases with micrometeorological methods. Ecology 69, 1331, http://dx.doi.org/10.2307/1941631
Baldocchi, D.D., Vogel, C.A., Hall, B., 1997. Seasonal variation of carbon dioxide exchange rates above and below a boreal jack pine forest. Agric. For. Meteorol. 83, 147–170, http://dx.doi.org/10.1016/S0168-1923(96)2335-0
Barford, C.C., Wofsy, S.C., Goulden, M.L., Munger, J.W., Pyle, E.H., Urbanski, S.P., Hutyra, L., Saleska, S.R., Fitzjarrald, D., Moore, K., 2001. Factors controlling long- and short-term sequestration of atmospheric CO_2 in a mid-latitude forest. Science 294, 1688–1691, http://dx.doi.org/10.1126/science.1062962
Binkley, D., Campoe, O.C., Gspaltl, M., Forrester, D.I., 2013. Light absorption and use efficiency in forests: why patterns differ for trees and stands? For. Ecol. Manage. 288, 5–13, http://dx.doi.org/10.1016/j.foreco.2011.11.002
Cheng, Y.-B., Zhang, Q., Lyapustin, A.I., Wang, Y., Middleton, E.M., 2014. Impacts of light use efficiency and fPAR parameterization on gross primary production modeling. Agric. For. Meteorol. 189–190, 187–197, http://dx.doi.org/10.1016/j.agrformet.2014.01.006
Crafts-Brandner, S.J., Law, R.D., 2000. Effect of heat stress on the inhibition and recovery of the ribulose-1,5-bisphosphate carboxylase/oxygenase activation state. Planta, 67–74, http://dx.doi.org/10.1007/s004250000364
Dall'Olmo, G., Gitelson, A.A., Rundquist, D.C., 2003. Towards a unified approach for remote estimation of chlorophyll-a in both terrestrial vegetation and turbid productive waters. Geophys. Res. Lett. 30, 1938, http://dx.doi.org/10.1029/2003GL018065
Desai, A.R., Richardson, A.D., Moffat, A.M., Kattge, J., Hollinger, D.Y., Barr, A., Falge, E., Noormets, A., Papale, D., Reichstein, M., Stauch, V.J., 2008. Cross-site evaluation of eddy covariance GPP and RE decomposition techniques. Agric. For. Meteorol. 148, 821–838, http://dx.doi.org/10.1016/j.agrformet.2007.11.012
Dwyer, L.M., Stewart, D.W., 1986. Effect of leaf age and position on net photosynthetic rates in maize (*Zea Mays* L.). Agric. For. Meteorol. 37, 29–46, http://dx.doi.org/10.1016/0168-1923(86)90026-2
El-Sharkawy, M.A., Cock, J.H., Held, K.A.A., 1984. Water efficiency of cassava. II. Differing sensitivity of stomata to air humidity in cassava and other warm-climate species. Crop Sci. 24, 503, http://dx.doi.org/10.2135/cropsci1984.0011183x002400030018x
Field, C., Mooney, H.A., 1983. Leaf age and seasonal effects on light, water, and nitrogen use efficiency in a California shrub. Oecologia 56, 348–355, http://dx.doi.org/10.1007/BF00379711
Fischer, R.A., 1921. On the probable error of a coefficient of correlation deduced from a small sample. Metron 1, 3–32.
Frank, J.M., Massman, W.J., Ewers, B.E., 2013. Underestimates of sensible heat flux due to vertical velocity measurement errors in non-orthogonal sonic anemometers. Agric. For. Meteorol. 171–172, 72–81, http://dx.doi.org/10.1016/j.agrformet.2012.11.005
Garbulsky, M.F., Peñuelas, J., Ogaya, R., Filella, I., 2013. Leaf and stand-level carbon uptake of a Mediterranean forest estimated using the satellite-derived reflectance indices EVI and PRI. Int. J. Remote Sens. 34, 1282–1296, http://dx.doi.org/10.1080/01431161.2012.718457
Gilmanov, T.G., Wylie, B.K., Tieszen, L.L., Meyers, T.P., Baron, V.S., Bernacchi, C.J., Billesbach, D.P., Burba, G.G., Fischer, M.L., Glenn, A.J., Hanan, N.P., Hatfield, J.L., Heuer, M.W., Hollinger, S.E., Howard, D.M., Matamala, R., Prueger, J.H., Tenuta, M., Young, D.G., 2013. CO_2 uptake and ecophysiological parameters of the grain crops of midcontinent North America: estimates from flux tower measurements. Agric. Ecosyst. Environ. 164, 162–175, http://dx.doi.org/10.1016/j.agee.2012.09.017
Gitelson, A.A., Keydan, G.P., Merzlyak, M.N., 2006. Three-band model for noninvasive estimation of chlorophyll, carotenoids, and anthocyanin contents in higher plant leaves. Geophys. Res. Lett. L11402, http://dx.doi.org/10.1029/2006GL026457, 33.
Gitelson, A.A., Peng, Y., Arkebauer, T.J., Schepers, J., 2014. Relationships between gross primary production, green LAI, and canopy chlorophyll content in maize: implications for remote sensing of primary production. Remote Sens. Environ. 144, 65–72, http://dx.doi.org/10.1016/j.rse.2014.01.004
Gu, L., Baldocchi, D.D., Verma, S.B., Black, T.A., Vesala, T., Falge, E.M., Dowty, P.R., 2002. Advantages of diffuse radiation for terrestrial ecosystem productivity. J. Geophys. Res. 107, 4050, http://dx.doi.org/10.1029/2001JD001242
Gu, L., Baldocchi, D.D., Wofsy, S.C., Munger, J.W., Michalsky, J.J., Urbanski, S.P., Boden, T.A., 2003. Response of a deciduous forest to the Mount Pinatubo eruption: enhanced photosynthesis. Science 299, 2035–2038, http://dx.doi.org/10.1126/science.1078366

Hall, F.G., Hilker, T., Coops, N.C., 2012. Data assimilation of photosynthetic light-use efficiency using multi-angular satellite data: I. Model formulation. Remote Sens. Environ. 121, 301–308, http://dx.doi.org/10.1016/j.rse.2012.02.007

Haxeltine, A., Prentice, I.C., 1996. A general model for the light-use efficiency of primary production. Funct. Ecol. 10, 551, http://dx.doi.org/10.2307/2390165

He, M., Ju, W., Zhou, Y., Chen, J., He, H., Wang, S., Wang, H., Guan, D., Yan, J., Li, Y., Hao, Y., Zhao, F., 2013. Development of a two-leaf light use efficiency model for improving the calculation of terrestrial gross primary productivity. Agric. For. Meteorol. 173, 28–39, http://dx.doi.org/10.1016/j.agrformet.2013.01.003

Held, L., Sabanés Bové, D., 2014. Applied Statistical Inference. Springer, Berlin Heidelberg, http://dx.doi.org/10.1007/978-3-642-37887-4

Hirasawa, T., Hsiao, T.C., 1999. Some characteristics of reduced leaf photosynthesis at midday in maize growing in the field. Field Crop Res. 62, 53–62, http://dx.doi.org/10.1016/S0378-4290(99)5-2

Inoue, Y., Peñuelas, J., 2006. Relationship between light use efficiency and photochemical reflectance index in soybean leaves as affected by soil water content. Int. J. Remote Sens. 27, 5109–5114, http://dx.doi.org/10.1080/01431160500373039

John, R., Chen, J., Noormets, A., Xiao, X., Xu, J., Lu, N., Chen, S., 2013. Modelling gross primary production in semi-arid Inner Mongolia using MODIS imagery and eddy covariance data. Int. J. Remote Sens. 34, 2829–2857, http://dx.doi.org/10.1080/01431161.2012.746483

Kalfas, J.L., Xiao, X., Vanegas, D.X., Verma, S.B., Suyker, A.E., 2011. Modeling gross primary production of irrigated and rain-fed maize using MODIS imagery and CO_2 flux tower data. Agric. For. Meteorol. 151, 1514–1528, http://dx.doi.org/10.1016/j.agrformet.2011.06.007

Kim, J., Verma, S.B., Clement, R.J., 1992. Carbon dioxide budget in a temperate grassland ecosystem. J. Geophys. Res. 97, 6057–6063, http://dx.doi.org/10.1029/92JD00186

Knohl, A., Baldocchi, D.D., 2008. Effects of diffuse radiation on canopy gas exchange processes in a forest ecosystem. J. Geophys. Res. 113, G02023, http://dx.doi.org/10.1029/2007JG000663

Kohavi, R., 1995. A Study of cross-validation and bootstrap for accuracy estimation and model selection. In: Mellish, C.S. (Ed.), International Joint Conference on Artificial Intelligence Lawrence Erlbaum Associates LTD. Montreal, Quebec, Canada, pp. 1137–1143.

Lasslop, G., Reichstein, M., Papale, D., Richardson, A.D., Arneth, A., Barr, A., Stoy, P., Wohlfahrt, G., 2010. Separation of net ecosystem exchange into assimilation and respiration using a light response curve approach: critical issues and global evaluation. Global Change Biol. 16, 187–208, http://dx.doi.org/10.1111/j.1365-2486.2009.02041.x

Leuning, R., van Gorsel, E., Massman, W.J., Isaac, P.R., 2012. Reflections on the surface energy imbalance problem. Agric. For. Meteorol. 156, 65–74, http://dx.doi.org/10.1016/j.agrformet.2011.12.002

Li, A., Bian, J., Lei, G., Huang, C., 2012. Estimating the maximal light use efficiency for different vegetation through the CASA model combined with time-series remote sensing data and ground measurements. Remote Sens. 4, 3857–3876, http://dx.doi.org/10.3390/rs4123857

Lobell, D.B., Hicke, J.A., Asner, G.P., Field, C.B., Tucker, C.J., Los, S.O., 2002. Satellite estimates of productivity and light use efficiency in United States agriculture. Global Change Biol. 8, 722–735, http://dx.doi.org/10.1046/j1365-2486.2002.00503.x

Mahadevan, P., Wofsy, S.C., Matross, D.M., Xiao, X., Dunn, A.L., Lin, J.C., Gerbig, C., Munger, J.W., Chow, V.Y., Gottlieb, E.W., 2008. A satellite-based biosphere parameterization for net ecosystem CO_2 exchange: Vegetation Photosynthesis and Respiration Model (VPRM). Global Biogeochem. Cycles 22, 1–17, http://dx.doi.org/10.1029/2006GB002735, GB2005.

Maselli, F., Papale, D., Puletti, N., Chirici, G., Corona, P., 2009. Combining remote sensing and ancillary data to monitor the gross productivity of water-limited forest ecosystems. Remote Sens. Environ. 113, 657–667, http://dx.doi.org/10.1016/j.rse.2008.11.008

Massman, W.J., 1991. The attenuation of concentration fluctuations in turbulent flow through a tube. J. Geophys. Res. 96, 15269, http://dx.doi.org/10.1029/91JD01514

Maurer, E.P., Wood, A.W., Adam, J.C., Lettenmaier, D.P., Nijssen, B., 2002. A long-term hydrologically based dataset of land surface fluxes and states for the conterminous United States. J. Clim. 15, 3237–3251, http://dx.doi.org/10.1175/1520-0442(2002)015<3237:ALTHBD>2.0.CO2

McCallum, I., Franklin, O., Moltchanova, E., Merbold, L., Schmullius, C., Shvidenko, A., Schepaschenko, D., Fritz, S., 2013. Improved light and temperature responses for light-use-efficiency-based GPP models. Biogeosciences 10, 6577–6590, http://dx.doi.org/10.5194/bg-10-6577-2013

Miyashita, K., Tanakamaru, S., Maitani, T., Kimura, K., 2005. Recovery responses of photosynthesis, transpiration, and stomatal conductance in kidney bean following drought stress. Environ. Exp. Bot. 53, 205–214, http://dx.doi.org/10.1016/j.envexpbot.2004.03.015

Monteith, J.L., 1972. Solar radiation and productivity in tropical ecosystems. J. Appl. Ecol. 9, 747–766, http://dx.doi.org/10.2307/2401901

Moreno, A., Maselli, F., Chiesi, M., Genesio, L., Vaccari, F., Seufert, G., Gilabert, M.A., 2014. Monitoring water stress in Mediterranean semi-natural vegetation with satellite and meteorological data. Int. J. Appl. Earth Obs. Geoinf. 26, 246–255, http://dx.doi.org/10.1016/j.jag.2013.08.003

Mu, Q., Heinsch, F.A., Zhao, M., Running, S.W., 2007. Development of a global evapotranspiration algorithm based on MODIS and global meteorology data. Remote Sens. Environ. 111, 519–536, http://dx.doi.org/10.1016/j.rse.2007.04.015

Mu, Q., Zhao, M., Running, S.W., 2011. Improvements to a MODIS global terrestrial evapotranspiration algorithm. Remote Sens. Environ. 115, 1781–1800, http://dx.doi.org/10.1016/j.rse.2011.02.019

Nakai, T., van der Molen, M.K., Gash, J.H.C., Kodama, Y., 2006. Correction of sonic anemometer angle of attack errors. Agric. For. Meteorol. 136, 19–30, http://dx.doi.org/10.1016/j.agrformet.2006.01.006

Narula, S.C., Saldiva, P.H., Andre, C.D., Elian, S.N., Ferreira, A.F., Capelozzi, V., 1999. The minimum sum of absolute errors regression: a robust alternative to the least squares regression. Stat. Med. 18, 1401–1417, http://dx.doi.org/10.1002/(SICI)1097-0258(19990615)18:11<1401::AID-SIM136>3.0.CO2-G

Nguy-Robertson, A.L., Gitelson, A.A., Peng, Y., Viña, A., Arkebauer, T.J., Rundquist, D.C., 2012. Green leaf area index estimation in maize and soybean: combining vegetation indices to achieve maximal sensitivity. Agron. J. 104, 1336–1347, http://dx.doi.org/10.2134/agronj2012.0065

Nguy-Robertson, A.L., Peng, Y., Gitelson, A.A., Arkebauer, T.J., Pimstein, A., Herrmann, I., Karnieli, A., Rundquist, D.C., Bonfil, D.J., 2014. Estimating green LAI in four crops: Potential of determining optimal spectral bands for a universal algorithm. Agric. For. Meteorol. 192–193, 140–148, http://dx.doi.org/10.1016/j.agrformet.2014.03.004

Norman, J.M., Arkebauer, T.J., 1991. Predicting canopy photosynthesis and light-use efficiency from leaf characteristics. In: Boote, K.J., Loomis, R.S. (Eds.), Modeling Crop Photosynthesis–from Biochemistry to Canopy. Crop Science Society of America, Madison, WI, pp. 75–94, http://dx.doi.org/10.2135/cssaspecpub19c5

Onoda, Y., Saluñga, J.B., Akutsu, K., Aiba, S., Yahara, T., Anten, N.P.R., 2014. Trade-off between light interception efficiency and light use efficiency: implications for species coexistence in one-sided light competition. J. Ecol. 102, 167–175, http://dx.doi.org/10.1111/1365-2745.12184

Pei, F., Li, X., Liu, X., Wang, S., He, Z., 2013. Assessing the differences in net primary productivity between pre- and post-urban land development in China. Agric. For. Meteorol. 171–172, 174–186, http://dx.doi.org/10.1016/j.agrformet.2012.12.003

Peltoniemi, M., Pulkkinen, M., Kolari, P., Duursma, R.A., Montagnani, L., Wharton, S., Lagergren, F., Takagi, K., Verbeeck, H., Christensen, T., Vesala, T., Falk, M., Loustau, D., Mäkelä, A., 2012. Does canopy mean nitrogen concentration explain variation in canopy light use efficiency across 14 contrasting forest sites? Tree Physiol. 32, 200–218, http://dx.doi.org/10.1093/treephys/tpr140

Peng, Y., Gitelson, A.A., Keydan, G.P., Rundquist, D.C., Moses, W., 2011. Remote estimation of gross primary production in maize and support for a new paradigm based on total crop chlorophyll content. Remote Sens. Environ. 115, 978–989, http://dx.doi.org/10.1016/j.rse.2010.12.001

Pettigrew, W.T., Hesketh, J.D., Peters, D.B., Woolley, J.T., 1990. A vapor pressure deficit effect on crop canopy photosynthesis. Photosynth. Res. 24, 27–34, http://dx.doi.org/10.1007/BF00032641

Prince, S.D., Goward, S.N., 1995. Global primary production: a remote sensing approach. J. Biogeogr. 22, 815, http://dx.doi.org/10.2307/2845983

Raich, J.W., Rastetter, E.B., Melillo, J.M., Kicklighter, D.W., Steudler, P.A., Peterson, B.J., Grace III, A.L.B.M., Vorosmarty, C.J., 1991. Potential net primary productivity in South America: application of a global model. Ecol. Appl. 1, 399, http://dx.doi.org/10.2307/1941899

Reich, P.B., Walters, M.B., Ellsworth, D.S., 1991. Leaf age and season influence the relationships between leaf nitrogen, leaf mass per area and photosynthesis in maple and oak trees. Plant Cell Environ. 14, 251–259, http://dx.doi.org/10.1111/j1365-3040.1991.tb01499.x

Richardson, A.D., Anderson, R.S., Arain, M.A., Barr, A.G., Bohrer, G., Chen, G., Chen, J.M., Ciais, P., Davis, K.J., Desai, A.R., Dietze, M.C., Dragoni, D., Garrity, S.R., Gough, C.M., Grant, R., Hollinger, D.Y., Margolis, H.A., McCaughey, H., Migliavacca, M., Monson, R.K., Munger, J.W., Poulter, B., Raczka, B.M., Ricciuto, D.M., Sahoo, A.K., Schaefer, K., Tian, H., Vargas, R., Verbeeck, H., Xiao, J., Xue, Y., 2012. Terrestrial biosphere models need better representation of vegetation phenology: results from the North American Carbon Program Site Synthesis. Global Change Biol. 18, 566–584, http://dx.doi.org/10.1111/j1365-2486.2011.02562.x

Running, S.W., Nemani, R.R., Heinsch, F.A., Zhao, M., Reeves, M., Hashimoto, H., 2004. A continuous satellite-derived measure of global terrestrial primary production. Bioscience 54, 547, http://dx.doi.org/10.1641/0006-3568(2004)054[0547:ACSMOG]2.0.CO2

Schwalm, C.R., Black, T.A., Amiro, B.D., Arain, M.A., Barr, A.G., Bourque, C.P.-A., Dunn, A.L., Flanagan, L.B., Giasson, M.-A., Lafleur, P.M., Margolis, H.A., McCaughey, J.H., Orchansky, A.L., Wofsy, S.C., 2006. Photosynthetic light use efficiency of three biomes across an east–west continental-scale transect in Canada. Agric. For. Meteorol. 140, 269–286, http://dx.doi.org/10.1016/j.agrformet.2006.06.010

Souza, R.P., Machado, E.C., Silva, J.A.B., Lagôa, A.M.M.A., Silveira, J.A.G., 2004. Photosynthetic gas exchange, chlorophyll fluorescence and some associated metabolic changes in cowpea (*Vigna unguiculata*) during water stress and recovery. Environ. Exp. Bot. 51, 45–56, http://dx.doi.org/10.1016/S0098-8472(03)59-5

Suyker, A.E., Verma, S.B., 2012. Gross primary production and ecosystem respiration of irrigated and rainfed maize–soybean cropping systems over 8 years. Agric. For. Meteorol. 165, 12–24, http://dx.doi.org/10.1016/j.agrformet.2012.05.021

Suyker, A.E., Verma, S.B., Burba, G.G., 2003. Interannual variability in net CO_2 exchange of a native tallgrass prairie. Global Change Biol. 9, 255–265, http://dx.doi.org/10.1046/j1365-2486.2003.00567.x

Suyker, A.E., Verma, S.B., Burba, G.G., Arkebauer, T.J., Walters, D.T., Hubbard, K.G., 2004. Growing season carbon dioxide exchange in irrigated and rainfed maize.

Agric. For. Meteorol. 124, 1–13, http://dx.doi.org/10.1016/j.agrformet.2004.01.011

Turner, D.P., Urbanskit, S., Bremert, D., Wofsyt, S.C., Meyers, T.P., Gower, S.T., Gregory, M., 2003. A cross-biome comparison of daily light use efficiency for gross primary production. Global Change Biol. 9, 383–395, http://dx.doi.org/10.1046/j1365-2486.2003.00573.x

Wang, X., Ma, M., Huang, G., Veroustraete, F., Zhang, Z., Song, Y., Tan, J., 2012. Vegetation primary production estimation at maize and alpine meadow over the Heihe River Basin, China. Int. J. Appl. Earth Obs. Geoinf. 17, 94–101, http://dx.doi.org/10.1016/j.jag.2011.09.009

Wang, Z., Xiao, X., Yan, X., 2010. Modeling gross primary production of maize cropland and degraded grassland in northeastern China. Agric. For. Meteorol. 150, 1160–1167, http://dx.doi.org/10.1016/j.agrformet.2010.04.015

Webb, E.K., Pearman, G.I., Leuning, R., 1980. Correction of flux measurements for density effects due to heat and water vapour transfer. Q. J. R. Meteorol. Soc. 106, 85–100, http://dx.doi.org/10.1002/qj.49710644707

Weiss, A., Norman, J.M., 1985. Partitioning solar radiation into direct and diffuse, visible and near-infrared components. Agric. For. Meteorol. 34, 205–213, http://dx.doi.org/10.1016/0168-1923(85)90020-6

Wofsy, S.C., Goulden, M.L., Munger, J.W., Fan, S.M., Bakwin, P.S., Daube, B.C., Bassow, S.L., Bazzaz, F.A., 1993. Net exchange of CO_2 in a mid-latitude forest. Science 260, 1314–1317, http://dx.doi.org/10.1126/science.260.5112.1314

Wu, W., Wang, S., Xiao, X., Yu, G., Fu, Y., Hao, Y., 2008. Modeling gross primary production of a temperate grassland ecosystem in Inner Mongolia, China, using MODIS imagery and climate data. Sci. China Ser. D Earth Sci. 51, 1501–1512, http://dx.doi.org/10.1007/s11430-008-0113-5

Xiao, X., 2006. Light absorption by leaf chlorophyll and maximum light use efficiency. Remote Sens. IEEE Trans. Geosci. 44, 1933–1935, http://dx.doi.org/10.1109/TGRS2006.874796

Xiao, X., Hollinger, D., Aber, J., Goltz, M., Davidson, E.A., Zhang, Q., Moore, B., 2004. Satellite-based modeling of gross primary production in an evergreen needleleaf forest. Remote Sens. Environ. 89, 519–534, http://dx.doi.org/10.1016/j.rse.2003.11.008

Xiao, X., Jin, C., Dong, J., 2014. Gross primary production of terrestrial vegetation. In: Hanes, J.M. (Ed.), Biophysical Applications of Satellite Remote Sensing. Springer, Heidelberg, New York, Dordecht, London, pp. 127–148, http://dx.doi.org/10.1007/978-3-642-25047-7_5

Xu, L., Baldocchi, D.D., 2004. Seasonal variation in carbon dioxide exchange over a Mediterranean annual grassland in California. Agric. For. Meteorol. 123, 79–96, http://dx.doi.org/10.1016/j.agrformet.2003.10.004

Yan, H., Fu, Y., Xiao, X., Huang, H.Q., He, H., Ediger, L., 2009. Modeling gross primary productivity for winter wheat–maize double cropping system using MODIS time series and CO_2 eddy flux tower data. Agric. Ecosyst. Environ. 129, 391–400, http://dx.doi.org/10.1016/j.agee.2008.10.017

Yuan, W., Liu, S., Yu, G., Bonnefond, J.-M., Chen, J., Davis, K., Desai, A.R., Goldstein, A.H., Gianelle, D., Rossi, F., Suyker, A.E., Verma, S.B., 2010. Global estimates of evapotranspiration and gross primary production based on MODIS and global meteorology data. Remote Sens. Environ. 114, 1416–1431, http://dx.doi.org/10.1016/j.rse.2010.01.022

Zhang, M., Yu, G.-R., Zhuang, J., Gentry, R., Fu, Y.-L., Sun, X.-M., Zhang, L.-M., Wen, X.-F., Wang, Q.-F., Han, S.-J., Yan, J.-H., Zhang, Y.-P., Wang, Y.-F., Li, Y.-N., 2011. Effects of cloudiness change on net ecosystem exchange, light use efficiency, and water use efficiency in typical ecosystems of China. Agric. For. Meteorol. 151, 803–816, http://dx.doi.org/10.1016/j.agrformet.2011.01.011.